The FEBS Journal

FEBS PRESS science publishing by scientists

STATE-OF-THE-ART-REVIEW

Cell cycle regulation by complex nanomachines

Marios G. Koliopoulos and Claudio Alfieri

Chester Beatty Laboratories, Structural Biology Division, Institute of Cancer Research, London, UK

Keywords
cell cycle; cryo-electron microscopy; structural biology; transcriptional regulation; ubiquitin

Correspondence
C. Alfieri, Chester Beatty Laboratories, Structural Biology Division, Institute of Cancer Research, 237 Fulham Road, London SW3 6JB, UK
Tel: +44 20715 35087
E-mail: claudio.alfieri@icr.ac.uk

(Received 5 February 2021, revised 5 May 2021, accepted 17 May 2021)

doi:10.1111/febs.16082

The cell cycle is the essential biological process where one cell replicates its genome and segregates the resulting two copies into the daughter cells during mitosis. Several aspects of this process have fascinated humans since the nineteenth century. Today, the cell cycle is exhaustively investigated because of its profound connections with human diseases and cancer. At the heart of the molecular network controlling the cell cycle, we find the cyclin-dependent kinases (CDKs) acting as an oscillator to impose an orderly and highly regulated progression through the different cell cycle phases. This oscillator integrates both internal and external signals via a multitude of signalling pathways involving posttranslational modifications including phosphorylation, protein ubiquitination and mechanisms of transcriptional regulation. These tasks are specifically performed by multisubunit complexes, which are intensively studied both biochemically and structurally with the aim to unveil mechanistic insights into their molecular function. The scope of this review is to summarise the structural biology of the cell cycle machinery, with specific focus on the core cell cycle machinery involving the CDK-cyclin oscillator. We highlight the contribution of cryo-electron microscopy, which has started to revolutionise our understanding of the molecular function and dynamics of the key players of the cell cycle.

Introduction

Orchestrating the cell cycle: switches, rheostats and oscillators

The basic biology of multicellular organisms crucially depends on the cell cycle. When a cell enters the cell cycle, it grows, replicates its genome and segregates the replicated sister chromatids into the dividing daughter cells (Fig. 1A). The core mechanism of the cell cycle is a background force in the development of multicellular organisms, tissue homeostasis and tissue repair upon injury. Misregulation of the cell cycle can lead to genetic mutations, which are the basis for human developmental disorders and cancer [1–3]. During cell cycle progression, the cell assumes distinct functional states or phases and the transition from one phase to the next is rapid, switch-like and unidirectional [4,5]. Each functional state is characterised by a unique cellular event, which is executed only once per cell cycle. During S-phase, the DNA replication is performed; during mitosis, the genome condenses in the structure of the mitotic chromosomes, and the replicated sister chromatids within each chromosome are segregated by the mitotic spindle into the daughter cells (Fig. 1A). Both the S and M phases are preceded by gap phases where the cell either grows and prepares for DNA synthesis (i.e. G1-phase), or prepares for mitosis (i.e. G2).

Abbreviations
APC/C, anaphase-promoting complex/cyclosome; CDKs, cyclin-dependent kinases; cryo-EM, cryo-electron microscopy; FBPs, F-box proteins; MCC, mitotic checkpoint complex; pRb, retinoblastoma protein; RBL, retinoblastoma-like protein; SAC, spindle assembly checkpoint; SCF, Skp1-cullin-F-box containing complex; SLiMs, short linear motifs.

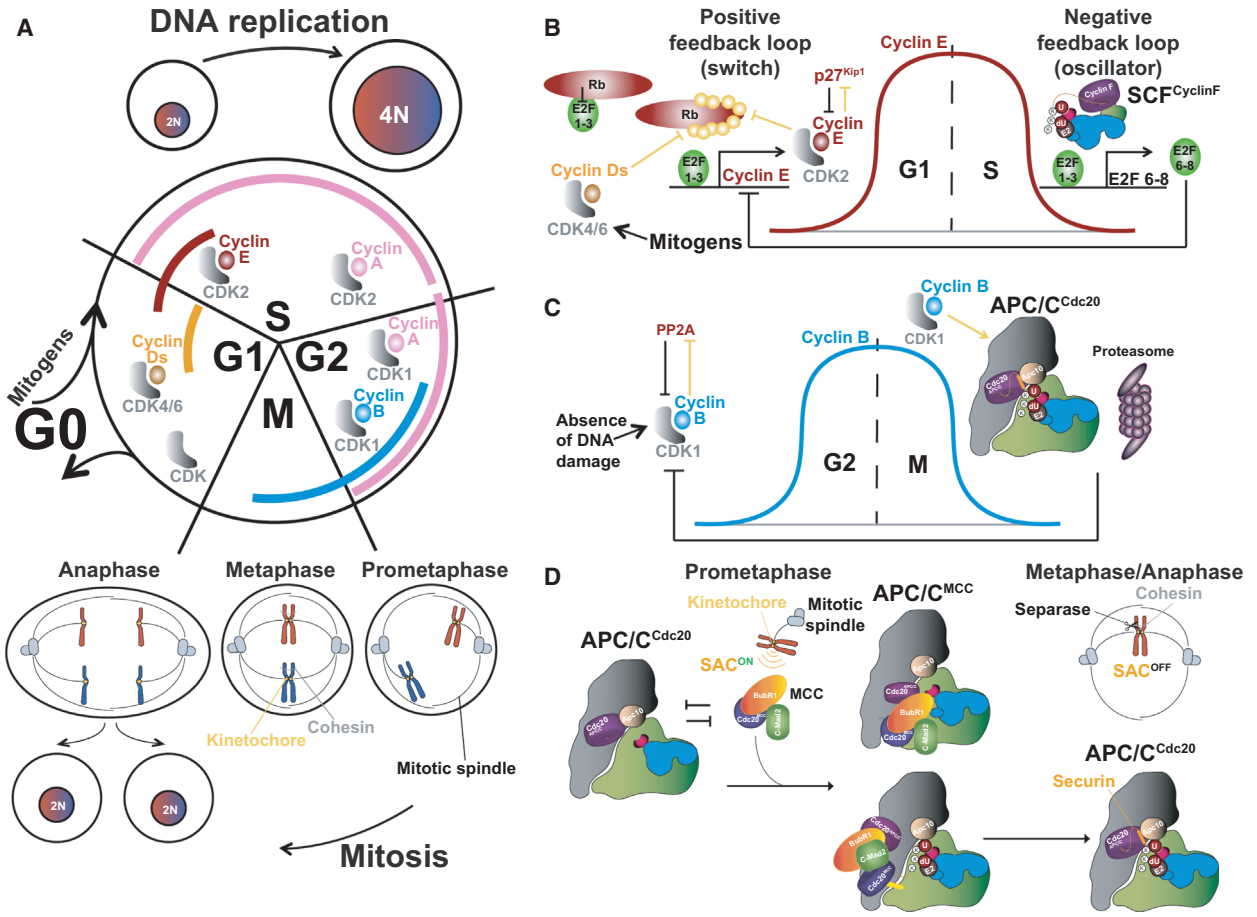

Fig. 1. The cell cycle and its key components are regulated by large molecular nanomachines. (A) Schematic cartoon illustrating the overview of the cell cycle phases (G1, S, G2 and M), along with the respective CDK-cyclin complexes which are necessary for cell cycle progression. The different phases within mitosis (M) are also represented. (B, C) Examples of bistable switches and oscillator systems regulating cell cycle transitions. Influence diagrams of the cell cycle regulators involved are also represented. Relevant macromolecular complexes are schematically represented: SCF and APC/C. The APC/C-coactivator Cdc20 is indicated. Switch-like cell cycle transitions feature a positive feedback loop that is turned off by a negative feedback loop, thereby causing the oscillations in cyclin levels. (B) In a simplified model, the G1/S transition is promoted by the positive feedback loop involving activating E2F1–3, CDK4/6-cyclin D and CDK2-cyclin E, which lead to the inactivation of the pRb by phosphorylation and to rising levels of cyclin E. This positive feedback loop is turned off by a negative feedback loop involving repressive E2F6–8 that are transcriptionally activated by the E2F1–3. Decreasing protein levels of E2Fs at the end of S-phase depend on their $SCF^{CyclinF}$-dependent ubiquitination and subsequent proteasomal degradation. $p27^{Kip1}$ inhibits the CDK2-cyclin E complex. (C) The G2/M switch (not shown for simplicity) is activated at the end of a successful S-phase, and results in rising levels of CDK1-cyclin B activity, which stimulates the APC/C activity. Cyclin B oscillation depends on its APC/C-dependant ubiquitination and subsequent proteasomal degradation during mitotic progression. Protein phosphatase 2A (PP2A) counteracts CDK1-cyclin B activity. (D) Cartoon showing the reciprocal regulation between the APC/C and the MCC. The MCC consisting of BubR1, Cdc20, active Mad2 (C-Mad2) [201] and Bub3 is assembled by the SAC at kinetochores which are improperly attached to the mitotic spindle. Two molecules of Cdc20 take part in the APC/C^{MCC} complex, one is the coactivator of the APC/C ($Cdc20^{APC/C}$) and the other is the inhibiting Cdc20 part of the MCC ($Cdc20^{MCC}$). The MCC is both inhibitor and substrate of the APC/C.

At the epicentre of the molecular network which controls the cell cycle, we find the cyclin-dependent kinases (CDKs) [6,7] (Fig. 1A). CDKs promote cell cycle transitions by phosphorylating specific downstream targets, which include the effectors of the cell cycle events. The activity of the CDKs oscillates in a cell cycle-specific manner according to the oscillating protein levels of the cyclin subunit which forms the active CDK-cyclin protein complexes. Cyclin proteostasis is primarily regulated by controlled protein degradation performed by the ubiquitin–proteasome system [8,9], and it involves two main classes of E3 ubiquitin ligases named the

Skp1-cullin-F-box containing complex (SCF) [10] and the anaphase-promoting complex/cyclosome (APC/C) [11,12] (Fig. 1B,C). Many more E3 ligases have been reported in the context of cell cycle regulation [13], although these findings seem to be confined to tumoral phenotypes, when, for example, the activity of the APC/C is reduced [14]. E3 ligases catalyse the polyubiquitination of protein substrates, thereby targeting them to the proteasome for proteolysis [15]. Moreover, cyclin genes are subjected to transcriptional regulation by multiple families of regulators including the E2F, the MuvB and the retinoblastoma proteins (pRb) [16]. Ultimately, the activity of the CDKs is regulated by cellular checkpoints, which delay a cell cycle transition until the cellular events of the previous cell cycle phase are successfully completed, in case of DNA damage [17], and within mitosis, in case of either incomplete or wrong assembly of the spindle [18].

Mathematical modelling efforts performed during the last decades reveal that cell cycle transitions are governed by bistable switches [19]. A bistable switch is a system that can adopt only two defined steady states and no intermediate states. In a bistable switch, the transition between the underlying states is characterised by a high degree of irreversibility [4].

Bistable switches govern the cell cycle entry decision (Fig. 1A,B). A cell is committed to divide from a reversible cell cycle arrest state named quiescence or G0 [20] when it is exposed to extrinsic signalling molecules called mitogens. This allows for increased transcription and subsequent increased protein levels of cyclin D that in conjunction with CDK4 and 6 phosphorylate and inactivate the pRb repressor. This repressor binds and inhibits the E2F transcriptional activators, thereby repressing the transcription of cell cycle genes. Once pRb is phosphorylated by CDK4 and 6, the E2F transcriptional programmes for S-phase entry are activated. Once mitogens stimulate the accumulation of a threshold level of CDK activity, the switch to S-phase is triggered irreversibly. This is due to the fact that CDK activity, inhibitory for pRb, is supported by a positive feedback loop where the E2Fs activate the transcription of cyclin E and cyclin A, which further strengthen CDK activity [21,22] (Fig. 1B). Importantly, the positive feedback loop triggering the cell cycle transition is coupled with a negative feedback loop, which completes the oscillation of CDK activity and avoids relicencing of replication origins [23,24] (Fig. 1B).

Entry into mitosis involves the counteracting activity of CDK1-cyclin B and the protein phosphatase PP2A [25] (Fig. 1C), and depends on the successful completion of DNA replication and on the absence of DNA damage, which switches off the G2/M checkpoint [17,26].

The molecular components that operate during mitotic progression and orchestrate the chromosome segregation process include the APC/C and its inhibitor, namely the mitotic checkpoint complex (MCC). The MCC is the effector of the spindle assembly checkpoint (SAC), a signalling cascade starting when kinetochores are improperly attached to the spindle microtubules [18,27–29] (Fig 1A,C,D). Chromosome segregation or anaphase is triggered by the APC/C-mediated ubiquitination and proteasomal degradation of two anaphase inhibitors, namely cyclin B [30] and Securin [31]. Securin degradation leads to the activation of its target Separase, which cleaves the Kleisin subunit of the cohesin complex [32]. This event relieves intrasister chromatid cohesion and triggers sister chromatid separation [33]. Cyclin B and Securin degradation spring up once all the chromosomes achieve correct bipolar attachments to the mitotic spindle. This event switches off the SAC and stops MCC production [18]. The APC/C is irreversibly activated because the MCC, apart from being an inhibitor, is also an APC/C substrate [34–36] (Fig. 1D). Since the strength of the SAC and its effects on delaying anaphase depend on the number of chromosomes with incorrect attachments to the spindle, the transition to anaphase is more rheostat-like, rather than switch-like [37,38].

In light of the above, biochemically speaking, the underlying components of any cell cycle switch function by establishing various protein–protein interactions, which impact on the subunit composition of the protein complex involved. Each key player of the cell cycle interacts with a multitude of inhibitory or activating modules, thereby forming a multitude of protein complexes with cell cycle-specific functions. An additional layer of regulation comes from the multitude of conformational states which characterises the key players of the cell cycle. For instance, at least four conformational states have been described as functionally relevant for the APC/C complex (reviewed in [39–41]). The scope of this review is to highlight the contribution of recent developments in structural determination by cryo-electron microscopy (cryo-EM) in elucidating the role of compositional and conformational heterogeneity in protein complexes regulating the cell cycle and discuss some perspectives in this exciting field.

Main sections

Structural methods for investigating the cell cycle machinery

Methods for studying the molecular biology of the cell cycle have been recently reviewed in Ref. [42]. High-

resolution structural studies of the cell cycle machinery have been classically performed by X-ray crystallography and NMR. Although these studies have been hugely impactful in the field, they are limited mainly to either rigid protein modules, or small domains, and these need to be purified in large quantities to homogeneity [43–45]. Conversely, cell cycle regulators often function in the context of large and complex protein assemblies which are often difficult to obtain in large amounts. Furthermore, these large complexes often adopt multiple structural conformations [41], and their components are engaged in transient interactions involving intrinsically disordered regions [46].

Strikingly, the latest revolutionary developments in cryo-EM [47,48] are now hugely enriching the field with high-resolution structures of large protein nanomachines where scaffolds, adaptors, substrates and catalytic modules are captured simultaneously while "in action," and while they perform their biochemical function [49]. In cryo-EM, a vitrified specimen is directly imaged on an EM support grid in the vacuum of an electron microscope. The electron beam that passes through the sample produces 2D projection images of fields of particles on a detector in a transmission electron microscope set-up. The recorded electron micrographs are fed into a single-particle analysis pipeline where images of individual particles are aligned together after determining their relative orientation. This produces 2D images with an improved signal-to-noise ratio. When the sample assumes random orientations on the grid, 2D images representative of different views are back-projected unto a 3D volume, which corresponds to the 3D reconstruction of the molecule of interest. The recent developments in both the hardware side and the software side of this pipeline allow the determination of high-resolution 3D reconstructions of the molecule of interest directly in solution, without the need to obtain protein crystals, and without the size limits imposed by NMR structural determination [50]. One major breakthrough in single-particle cryo-EM has been the introduction of direct-electron detection cameras with high detective quantum efficiency (DQE). These cameras can run at high frame rate, thereby allowing the recording of cryo-EM images as movie stacks, which can be corrected for beam-induced motion. This correction alleviates the effects of radiation damage. The other major breakthrough came from the new image processing algorithms, which allow to classify structural heterogeneity *in silico* and greatly improve the accuracy of image alignment of all the particles used to reconstruct the density map [47].

In the following paragraphs, we attempt to summarise the structural biology of the cell cycle core components and highlight, where possible, the contribution of single-particle cryo-EM in helping to decipher the molecular function of this system.

Cyclin-CDK complexes in cell cycle progression

CDK-cyclin complexes form a large family of heterodimeric serine/threonine protein kinases involved in controlling progression through the cell cycle [51], with some families also involved in gene regulation [52]. The CDK activity is counteracted by protein phosphatase complexes, which are reviewed in Ref. [53]. CDK proteins are defined by a catalytic core comprising the ATP-binding pocket, the PSTAIRE-like cyclin-binding domain and an activating T-loop motif [54] (Fig. 2A). The active site of a monomeric CDK is blocked by a glycine-rich loop in the N-terminal lobe which buckles the activation loop hanging from the C-terminal lobe [55] (Fig. 2A). Cyclin binding repositions the PSTAIRE motif-containing αC helix that results in a repositioning of the αL12 helix at the start of the activation loop [56] (Fig. 2B). Due to this, the activation loop loosens the interaction with the glycine-rich loop and it opens up. Phosphorylation at Threonine 160 by the master cyclin-activating kinase (CAK) induces melting of the αL12 helix. The latter causes a further rearrangement of the activating loop, which augments its interactions with the cyclin, thereby allowing the formation of a complete active site [57] (Fig. 2C). Although this mechanism of CDK activation is conserved between CDK2-cyclin A and CDK1-cyclin B complexes [58], the CDK4-cyclin D complex features a distinct activation mechanism that involves a phosphorylated form of the CDK inhibitor (CKI) $p27^{Kip}$. In a landmark study from the Rubin lab, the crystal structure of a CDK4-cyclin D complex with phospho-$p27^{Kip}$ shows that $p27^{Kip}$ is required for shaping the CDK4 catalytic site and that nonreceptor tyrosine kinase (NRTK)-mediated phosphorylation of $p27^{Kip}$ relieves the inhibition on the ATP-binding site. This activation is required for pRb phosphorylation. Importantly, this effect is specific for CDK4, and not for CDK2 where $p27^{Kip}$ functions exclusively as an inhibitor [59].

Cyclin proteins are defined by a ~ 100-residue-long sequence called cyclin box. This region folds in a conserved domain consisting of one central helix (α3) surrounded by the remaining α1, 2, 4 and 5 (Fig. 2D). Two copies of this structural domain are often present in tandem. The cyclin box is also present in other cell cycle regulators described later in the text such as the retinoblastoma transcriptional regulators [60] (Fig. 2E). More N-terminally to the cyclin box, both S

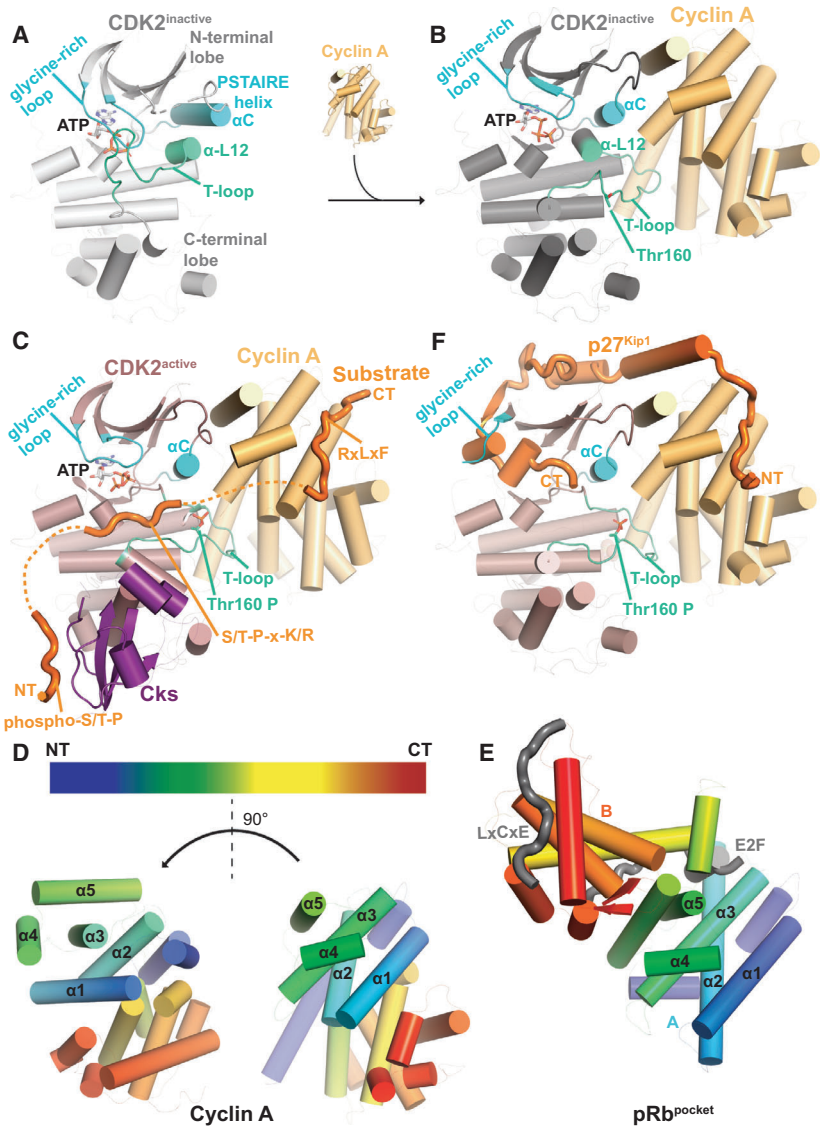

Fig. 2. Structural overview of CDK-cyclin complexes. (A) Ribbon model of the monomeric CDK2 (PDB ID: 1HCK) crystal structure. In the absence of cyclin, CDK is autoinhibited. Segments relevant for autoinhibition and activation are depicted. For clarity, unmentioned loops are not shown and helices are represented as cylinders. (B) Crystal structure of CDK2-cyclin A complex (PDB ID: 1FIN). Upon cyclin binding, conformational changes lead to partial release of inhibition. (C) Crystal structure of the $CDK2^{pThr160}$-cyclin A complex (PDB ID: 1JST). Thr160 phosphorylation fully activates the CDK-cyclin complex as described in the main text. In this model, also a full CDK substrate is depicted by the superposition of PDB IDs: 2CCI, 1BUH and 4LPA. Substrate recognition involves multiple recognition sites with cyclin, CDK and cofactor Cks all contributing to substrate positioning into the catalytic cleft of CDK. (D) Two different views of the cyclin A model from (B) are shown with rainbow colour code, according to their position along the N terminus to C terminus direction of the polypeptide chain. The colour code is specified as a scale bar indicated on top. (E) Crystal structure of the pRb pocket domain (PDB ID: 1N4M). The N-terminal cyclin box fold was superposed to the corresponding fold from the structure in (D). Peptide-interacting motifs relevant for the pRb function are depicted. The cyclin fold is conserved across all eukaryotes, and it is also present in the Retinoblastoma family of proteins. The orientation of N- and C-terminal cyclin box folds in cyclin A and pRb is different. (F) Crystal structure of CDK2-cyclin A-$p27^{Kip1}$ complex (PDB ID: 1JSU). $p27^{Kip1}$ competes with substrate recognition by masking the CDK active site and the substrate-binding region on the cyclin subunit.

and M-phase cyclins contain short linear motifs (SLiMs) called degrons that serve as recognition motifs for the APC/C and are required for their APC/C-mediated ubiquitination and proteasomal degradation during mitosis. SLiMs relevant in cell cycle regulation are reviewed in Ref [46].

Substrate recognition involves the CDK active site which recognises the consensus S/T-P-x-K/R sequence [61], a conserved patch on the cyclin subunit which is specific for the RxLxF motif [62], and an accessory subunit named Cks which recognises phosphorylated S/T-P motifs [63–66] (Fig. 2C) [66]. CKIs such as $p27^{Kip1}$ compete with CDK substrates by tightly binding to the substrate recognition sites on the CDK and cyclin subunits. Moreover, $p27^{Kip1}$ inhibits ATP binding and deform the catalytic site of CDK. [67] (Fig. 2F). $p27^{Kip1}$ is considered a marker of quiescent cells [68]; conversely, $p21^{Cip1}$ is associated with quiescence induced after DNA damage occurring during the previous cell cycle [69].

Our current view of CDK activation and substrate recognition for the cell cycle-related CDKs is mainly based on a subset of CDK-cyclin complexes [58,59,70,71], which are excellent targets for crystallisation in different phosphorylation states and in complex with several types of inhibitors. Extending these studies to other cell cycle regulating CDK complexes and to CDK-substrate complexes will be critical to augment our mechanistic view on substrate recognition and regulation of this class of enzymes during cell cycle progression. Recently, Greber *et al.* [72,73] demonstrated that cryo-EM methods can be employed to determine high-resolution structures of CDK-cyclin complex refractory to crystallisation. In this study, the structure of the human CAK, comprising CDK7, cyclin H and the assembly factor MAT1, was determined by single-particle cryo-EM. This structure shows that, contrary to the CDK2-cyclin A complex, the C-terminal cyclin fold of cyclin H and the C-terminal lobe of CDK7 are rotated away from each other, thereby vacating a space occupied by MAT1, which stabilises the overall complex assembly. The study has huge potential in expanding the possibilities of anticancer drug design targeting the CDK-cyclin complexes [73–76]. Moreover, this system can also be employed to study highly dynamic processes such as the CAK-dependent activation of the downstream CDK-cyclin complexes.

Furthermore, a cryo-EM structure of CDK4 in complex with Hsp90-Cdc37 has provided key insights into CDK4 maturation, another highly dynamic process [77].

SCF complexes in interphase regulation

Timely protein degradation of cell cycle regulators depends on the concerted action of multi-subunit E3 ubiquitin ligases belonging to the family of cullin-RING ligases (CRLs). These E3s are responsible for timely 'culling' cyclins, CKIs and a plethora of other proteins via the proteasome, thus allowing cell cycle progression. CRLs account for ~ 20% of all proteasomal degradation [13,78,79]. During the last 20 years, seminal studies on the CRLs have shed light on their core complex assembly, interactions with substrates and activation/inactivation mechanisms. Due to its key role in cell cycle, early structural studies were focused on a subfamily of CRLs, the Skp1-Cul1-F-Box-protein or SCF E3 ubiquitin ligase which formed the archetypical member of the CRLs [80,81] (Fig. 3A). Cul1 forms an elongated α-helical repeat-containing scaffold where the N terminus interacts with the adaptor module S-phase-kinase-associated protein-1 (Skp1). Skp1 interacts with the F-box domain of one F-box protein (FBP) that act as substrate receptors [82]. The C terminus of Cul1 forms a globular complex with the catalytic RING domain (RBX1) which is responsible for recruiting and activating a ubiquitin-loaded E2 conjugating enzyme (Fig. 3A).

The structural basis of the Cul1-RBX1 interaction involves a Cul1 cavity formed by a four-helical bundle, which extends into an α/β domain nesting an RBX1 β-strand. The latter is further stabilised by two Cul1 winged-helix motifs, namely WHA and WHB (Fig. 3A). In this arrangement, revealed by X-ray crystallography, the active module (the C-terminal Cul1-RBX1 subcomplex) is located more than 50 Å apart from the substrate-binding module at the N terminus [82]. Many studies showed that in this orientation, the SCF complex and many other CRLs are in an inactive conformation. This conformation is further stabilised by the binding of another factor, CAND1 [83,84]. CAND1 'hugs' Cul1, thereby sterically inhibiting interactions with Skp1 and the F-box substrate receptors [84].

The activity of CRLs is stimulated by the covalent attachment of NEDD8, a ubiquitin-like modification [85,86]. NEDD8 ligation competes with binding of CAND1, thereby shifting the equilibrium towards an active SCF E3 complex [83,86]. A highly conserved lysine residue within the WHB domain is the target of this reversible NEDD8 modification [86]. NEDD8 induces large conformational changes allowing the RING domain to move closer to the substrate receptor and its bound target protein. A more definite structural model of this was only possible through the use of cryo-EM [83,86–88] (Fig. 3B). In this study, a snapshot of the ubiquitin-transfer onto a phosphorylated substrate recruited through an FBP was obtained, and the key role of covalently attached NEDD8 into inducing large structural changes on Cul1 was finally revealed [87]. NEDD8 acts as a hub of interactions

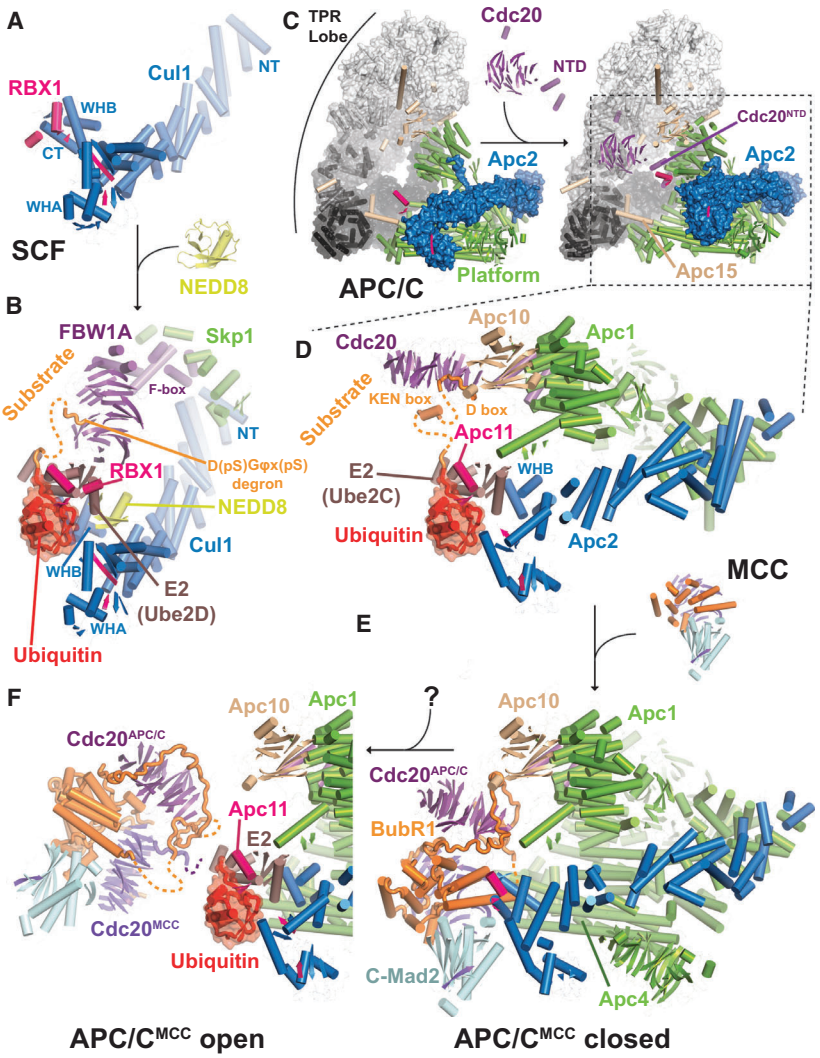

Fig. 3. Cryo-EM-obtained snapshots of active E3 ubiquitin ligases regulating cell cycle progression. (A) Ribbon model of the Cul1-RBX1 crystal structure (PDB ID: 1LDJ). Cul1 forms an elongated platform in which the RING-containing RBX1 protein is embedded. (B) Ribbon model of the $Cul1^{NEDD8}$-RBX1-Skp1-FBW1A complex cryo-EM structure (PDB ID: 6TTU). Upon NEDD8 (yellow) attachment onto Cul1 (blue), structural rearrangements bring a Lys residue of an FBP-bound substrate (orange) in close proximity to the E2-activated ubiquitin (brown and red, respectively) providing a snapshot of SCF-mediated substrate ubiquitination. FBW1A (purple) recognises its substrates through a D(pS)Gφx(pS) phosphodegron where φ is a hydrophobic and x can be any residue. (C) Model of the cryo-EM structure of the APC/C complex in the absence (left) and in complex with its coactivator Cdc20 (right). PDB ID codes are 5G05 and 5G04, respectively. For facilitating visualisation, the TPR lobe is shown in transparent surface representation (grey colours) and only one TPR monomer per TPR dimer is shown as cartoon representation. The platform subcomplex is shown in green. The rearrangement induced by coactivator binding on the catalytic site (Apc2 and Apc11) conformation is shown. (D) Close-up of the APC/C catalytic site and substrate recognition modules, showing a snapshot of the E3 ligase reaction (PDB ID: 5A31). Ubiquitin (red) in closed conformation is modelled. Upon Cdc20 coactivator binding, APC11 RING domain becomes accessible for E2~Ubiquitin binding and the substrate is primed for ubiquitination. Colour code for cullin subunit (blue), RING protein (red), substrate receptor (purple), substrate (orange), ubiquitin (red), E2 (brown) and adaptor module (green) is the same as in figure (B) to facilitate comparisons. (E) Close-up on the APC/C catalytic site and substrate recognition modules, showing an APC/C-Cdc20 complex inhibited by the MCC complex (PDB ID: 6TLJ). The MCC complex can act as a pseudosubstrate inhibitor of the APC/C via its subunit BubR1 (orange). In the APC/C^{MCC} closed conformation, (E) BubR1 occlude the E2-binding site on Apc2 and 11, thereby inhibiting ubiquitin chain initiation. In the APC/C^{MCC} open conformation, (F) the MCC module is moved away from Apc2 and 11, which allows E2~Ub binding and the MCC is primed for ubiquitination. How the open/closed state equilibrium is regulated in the cell is unknown and this is indicated with a question mark.

between different parts of the Cul1 protein but also enhances the active E2~Ub closed conformation by making contact with the so-called 'backside' of the E2 [87] (Fig. 3B). These interactions allow the RING domain to become mobile and prime the E2~Ub for transfer onto the juxtaposed substrate. Single-particle cryo-EM has also provided snapshots of how a related multi-subunit complex, the COP9-signalosome (CSN) binds to and removes the NEDD8 moiety from the SCF complex thereby inactivating it [89,90].

SCF complexes rely on nearly 70 FBPs for substrate recruitment, allowing them to polyubiquitinate very diverse protein substrates related to the cell cycle but also to every other aspect of eukaryotic biology [81,91,92]. Apart from the cullin protein being regulated by posttranslational modifications (i.e. NEDD8 attachment), an additional layer of control is exerted on substrate recruitment. FBPs recognise their substrates in multiple ways. Initially, a degron that bears a phosphorylated residue (phosphodegron) was considered the paradigm for SCF substrate recruitment. However, as more FBPs were paired with their respective substrates, it became evident that this rule has many exceptions, some of which are discussed below [92].

The founding member of the FBPs, cyclin F, is the largest cyclin protein, and its protein levels oscillate throughout the cell cycle. As the name suggests, it contains a cyclin domain and, importantly, also a small ~ 40 residue motif which the Elledge lab named F-box [91,93]. This F-box is responsible for the interaction with the adaptor protein Skp1 as part of the SCF [94] (Fig. 3B). Cyclin F differs from the canonical cyclin-CDK paradigm as it does not activate a CDK and plays no role in phosphorylating a substrate [95]. Similar to other cyclins, the cyclin fold of cyclin F interacts with target proteins through an RxLxF-like motif that in this context acts as a degron for polyubiquitination by the SCF-cyclin F complex and subsequent proteasomal degradation [92,95]. The majority of the validated SCF-cyclin F substrates are involved in cell cycle regulation. Among them, we find the APC/C-coactivator Cdh1, which is also an APC/C substrate [95,96]. This contributes to inactivating the APC/C during late G1-phase and allows for S-phase entry. Interestingly, in a double negative feedback loop control, APC/C is targeting cyclin F for degradation through the Cdh1 component in early G1-phase [96].

Following the discovery of cyclin F, other proteins that contain the F-box at their N terminus were identified. As in the case of cyclin F, these proteins form distinct SCF complexes through a direct interaction with Skp1 [81,92]. FBPs are categorised into three main classes, depending on the structural fold at their respective C terminus which mediates the protein–protein interaction with the E3 ligase substrate. FBXW are FBPs that contain a WD40 domain, FBXL contain a Leu-rich repeat (LRR) and FBXO proteins, including cyclin F, have miscellaneous or 'Other' domains [91] (Fig. 3B).

Skp2 (S-phase kinase-associated protein 2, also known as FBXL1) remains one of the best characterised FBPs, both functionally and structurally. It is well established that Skp2 is overexpressed in numerous human cancers [97]. Skp2 plays a key role in the G1/S transition as it targets CKIs of the Cip/Kip family (namely $p21^{Cip1}$, $p27^{Kip1}$, $p57^{Kip2}$) that interfere with the activity of cyclin A-, B-, D-, E-dependent kinase complexes [98,99]. In another negative feedback inhibition example, $p27^{Kip1}$ is phosphorylated by CDK2-cyclin A/E on Thr187 [100]. This allows recognition of the $p27^{Kip1}$ phosphodegron by the SCF^{Skp2} and leads to its ubiquitination with the help of the accessory subunit Cks1 [99,101]. The crystal structure of the Skp1-Skp2-Cks1 complex bound to the $p27^{Kip1}$ phosphodegron showed that Skp2 interacts with Skp1 through a canonical F-box interaction, whereas the LRR motif of Skp2 embraces mainly Cks1 that in turn binds the pThr187 of $p27^{Kip1}$ [92,101]. Another Skp2 substrate is retinoblastoma-like protein 2 (RBL2; also known as p130), a retinoblastoma-like 'pocket protein' which binds to and restricts activity of E2F transcription factors [102–104]. As quiescent cells re-enter the cell cycle, RBL2 is phosphorylated by cyclin D-CDK4/6 leading to a conformational change and release from the RBL2-E2F repressive complexes [102,105]. This phosphorylated form of RBL2 is then recognised by SCF-Skp2 in complex with Cks1 and is subsequently ubiquitinated and degraded [103,104]. Future structural studies will show whether Cks1 plays a similar role in RBL2 recognition by SCF-Skp2 as it does for the recognition of $p27^{Kip1}$.

Another SCF E3 ligase with a distinct mechanism of substrate recruitment is SCF-FBXW7 which polyubiquitinates cyclin E, the activating partner of CDK2, at the G1/S boundary [106,107]. Structural analysis of the Skp1-FBXW7-cyclin E complex shows that the WD40 domain of FBXW7 can recognise two different phosphodegrons of cyclin E: a doubly phosphorylated pThr380/pSer384 peptide and a mono-phosphorylated peptide around pThr62 [108]. Crystal structures of the Skp1-FBXW7 complex bound to the two cyclin E phosphodegrons showed that each phosphopeptide occupies the same binding site on top of the main FBXW7 WD40 cavity [108]. The authors additionally showed that FBXW7 can dimerise, raising an

interesting avidity-driven model of E3 ligase action where two SCF-FBXW7 complexes bind one cyclin E substrate through its two phosphodegrons leading to increased processivity [108]. Future studies are required to understand how the two E3s cooperate to effectively ubiquitinate a single substrate and why this is required, given that SCF E3 enzymes are highly processive even when stoichiometric to their substrate. Along this line, a recently published study reveals another insight into this SCF substrate pair and another E3 ligase, named ARIH1, which is required for efficient ubiquitination of cyclin E [109–111]. A series of cryo-EM structures show that ARIH1 binds to the Cul1-RBX1 interface creating an E3–E3 superassembly where ARIH1 transfers the ubiquitin to the substrate, while SCF has no catalytic role in this instance [111]. The authors suggest that ARIH1 may compensate for substrates that are bulkier or show less mobility, a situation where a conventional SCF-only catalysis is less effective.

Proteins from the FBXO family [91] remain largely uncharacterised both in terms of their substrates but also structurally. Recent structural studies have revealed unique-binding domains, such as the double β-barrel motifs of FBXO31 that interact with a phosphodegron of cyclin D1 as part of the DNA damage response [112,113]. This structure begins to highlight the structural diversity of FBPs and further hints to the need for further characterisation of other SCF E3s, given the tumour-suppressive or oncogenic functions of many FBPs [114].

Within the last two decades, the majority of the structural knowledge on the SCF E3 ligases came from X-ray crystallography [81]. However, single-particle cryo-EM has recently contributed with further answers to long-standing questions regarding the structural rearrangements and the activation/inactivation mechanisms of the CRL E3 complexes [87–90,111]. With cryo-EM methods now streamlined and further improving at a fast pace, it is possible that we will soon have further insights into ubiquitination mediated by SCFs. How do different E2s coordinate ubiquitination? How does the conformation of the substrate-bound SCF complex change to accommodate ubiquitin chain elongation? Does the size and shape of the substrate affect SCF polyubiquitination and is there any correlation with the FBPs? What is the role of SCF oligomerisation in enhancing substrate ubiquitination? What is the optimal positioning (if there is an optimum) and number of lysines at the ubiquitination sites? Why very often only one partner in a multiprotein complex gets ubiquitinated and degraded, while the others remain untouched? These are some of the questions we anticipate will be answered in the near future and might further help in the development of novel therapeutics, including proteolysis-targeting chimeras that bridge E3s with non-native, medically important substrates for degradation [115].

APC/C complexes in mitotic progression

The APC/C is an unusually large cullin-RING E3 ubiquitin ligase. Structural efforts performed during the last decades, which involved also the latest developments in cryo-EM unveiled an extremely complex and dynamic cell cycle regulator [39–41,116]. Similar to the SCF complex, the APC/C features a catalytic module comprising a cullin subunit (Apc2) which binds a RING domain protein (Apc11) via its C terminus [117] and a substrate receptor protein named coactivator involved in substrate recognition [39,118] (Fig. 3A–D). Cdc20 is the coactivator required for recognising the APC/C mitotic substrates cyclin B and Securin. Conversely, the coactivator Cdh1 is required for recognising substrates that are degraded later in the cell cycle, such as Cdc20 during mitotic exit and cyclin F in G1-phase [96]. The former is essential for the execution of mitotic exit, establishment of G1 and quiescence (G0) [119–121]. The molecular details on how the APC/C-coactivator complexes recognise target substrates have been reviewed extensively [39,46], and it involves specific SLiMs on target substrates, namely the D box [8], KEN box [122] and ABBA motifs [123,124]. These motifs are recognised by distinct patches on the coactivator WD40 domain [39]. The D box is recognised by a coreceptor involving the coactivator and the Apc10 core subunit [125]. Another SLiM named MR motif is coactivator-independent [126–129]. Similarly to SCF, the APC/C recognises phosphodegron motifs as reviewed in Ref. [39]. When comparing the APC/C with other E3 ligases, it is quite striking to notice that the adaptor module connecting the catalytic site with the substrate receptor is an unusually large and complicated protein scaffold forming a central cavity [117] (Fig. 3C). This adaptor module allows substrate recognition and catalysis to happen in a confined and highly regulated environment [39,130–132]. The APC/C adaptor module is composed of a so-called tetratricopeptide repeat (TPR) [133] lobe and a platform module (Fig. 3C). The platform module includes the largest subunit of the APC/C called Apc1, which, together with Apc4, recruits the catalytic module [117,128] (Fig. 3C). The TPR lobe is composed of TPR-containing homodimers which stack on top of each other, thereby forming a TPR superhelix. The TPR lobe, in synergy with the platform, recruits the

coactivator subunit via specific 'hook'-like dipeptide motifs containing an arginine and a hydrophobic residue [39,46]. One of these motifs, namely C box, is located on the N-terminal domain (NTD) of the coactivator and binds the APC/C in a cleft, right at the centre of the APC/C cavity between Apc1 and the Apc8 homodimer B, at the interface between platform and TPR lobe [117] (Fig. 3C). As shown by cryo-EM, this interaction induces a remarkable conformational change on the catalytic site. Here, the Apc2 C terminus and Apc11 are lifted upwards from the platform, thereby exposing the recruitment site for the E2 enzyme [132,134] (Fig. 3C,D). As in the SCF complex, the E2 contacts the C-terminal WHB domain of the cullin subunit Apc2 and the RING domain of Apc11 (Fig. 3A–D).

Recent cryo-EM studies have shown that the complex of APC/C with the mitotic coactivator Cdc20 and its inhibitor complex MCC features striking conformational flexibilities [131,135]. In one conformation named APC/C^{MCC} closed, the MCC blocks substrate recognition by obstructing the APC/C substrate recognition sites with specific pseudosubstrate sequences present in the MCC protein named BubR1 (Figs 1D and 3D,E). Furthermore, in APC/C^{MCC} closed, the MCC obstructs the E2 enzyme-binding site thereby competing with the E2 and inhibiting ubiquitin chain initiation (Fig. 3D,E). In another conformer named APC/C^{MCC} open (Fig. 3F), the MCC module is rotated in such a way that the catalytic inhibition is released and the binding of both the MCC and the E2 becomes possible within the same molecule of APC/C. In this complex, the MCC switches from an APC/C inhibitor to an APC/C substrate [131,135]. Pioneering work has demonstrated that the MCC is indeed ubiquitinated by the APC/C during mitosis in a cellular context and that this process depends on the small subunit called Apc15 [34–36] (Fig 3C). Removal of Apc15 locks APC/C^{MCC} in closed conformation [131,135] and prolongs mitosis [36]. These data support a fascinating model where the APC/C^{MCC} enzyme is not fully inhibited. The APC/C^{MCC} is capable of binding the E2 enzyme and promoting the ubiquitination of its own inhibitor MCC. This allows the APC/C to act as a 'sensor' of the MCC levels produced at kinetochores, where the APC/C activity against its mitotic substrates is delayed by the MCC, which functions as a competitive inhibitor substrate, until there are no unattached kinetochores left. Once the attachments are complete, the APC/C will extensively ubiquitinate the MCC, which leads to MCC disassembly [136]. Then, the APC/C-Cdc20 will readily ubiquitinate cyclin B and Securin for triggering anaphase (Fig. 1A,D). Even though this model is tempting and would help explain how anaphase is synchronised with the assembly of the spindle, it lacks experimental validation *in vivo*. For example, it will be critical to assess whether mutations that promote the APC/C^{MCC} open state could accelerate mitosis in an opposite fashion to Apc15 depletions. It is also critical to understand how the APC/C^{MCC} closed to open transition is regulated in the cell by post-translational modifications such as phosphorylation or SUMOylation.

In conclusion, cryo-EM has been an excellent tool for exploring the APC/C complex assembly and conformational variability. The cryo-EM studies on the APC/C^{MCC} represent an example of how EM allows to visualise multiple conformations within a single sample preparation, thereby providing snapshots of a 'nanomachine in action'. These structural data can now be used for generating new hypotheses to probe the APC/C function during mitotic progression *in vivo*.

Transcriptional complexes in cell cycle regulation

The majority of cell cycle-specific genes are transcriptionally regulated by multiple families of regulators including the E2F, B-MYB, FOXM1 transcription factors, the retinoblastoma 'pocket proteins' and the multivulva class B (MuvB) complex [16,23]. There are eight human *E2F1-E2F8* genes which encode several protein products due to expression from alternative promoters (such as *E2F3a and b*) and alternative splicing (*E2F7*) [23,137]. Every E2F protein contains a conserved DNA-binding domain (DBD) that engages its target gene promoters at a similar consensus DNA sequence. E2Fs can be classified based on their transcriptional capacity, with some being activators (E2F1, E2F2, E2F3a) and some repressors (E2F3b, E2F4-E2F8) [23,137–139]. In a rather simplified model of E2F function, oscillations in cell cycle-regulated gene expression derive from sequential action of both E2F activators and suppressors [137,140] (Fig. 1B).

The E2F transcriptional oscillator is intertwined with the protein oscillator dictated by the SCF and APC/C E3s [141]. The SCF-cyclin F E3 ligase is responsible for degrading the transcriptional activators E2F1–3a in late S-phase and after DNA replication, whereas the APC/C-Cdh1 targets the repressive E2F7–8 during G1, thereby allowing levels of E2F1-E2F3a to increase and initiate another round of DNA replication [141–144]. Furthermore, targeting of E2F7–8 during G2 by SCF-cyclin F is required for DNA repair after DNA replication [145].

Additionally, the activity of E2Fs is modulated by protein–protein interactions. E2F1–6 bind to dimerization

partners (DP1, DP2, DP3) whereas E2F7–8 need to homo/heterodimerise for DNA binding [137,139,141]. Importantly, E2F1-E2F5 proteins also contain a transactivation domain that either recruits transcriptional coactivators or one of the three RB proteins namely pRB, and the RB-like proteins RBL1/p107 or RBL2/p130. RB proteins mask the E2F transactivation domain, thereby repressing its transcriptional activating function [137,146,147]. The RB family of proteins are key components of the cell cycle. However, their bistable switch controlling E2F-mediated transcription and cell cycle progression [102,148] is often inactivated in cancerous cells [149]. All three RB proteins share a similar architecture, with a central domain that is termed 'pocket' region because, within this fold, a pocket embeds the E2F transactivation domain. The pocket is flanked by an N-terminal (RB-N) [150] and a C-terminal domain (RB-C) [151] (Figs 2E and 4B). Both the pocket domain and the RB-N are structurally composed of two flexibly linked subdomains, A and B, which bear structural homology to the cyclin box fold [150,152] (Fig. 2E). The pocket domain interacts with a plethora of RB-binding proteins, including the E2F transactivation domain of the E2F-DP complex, the Cdh1 substrate receptor of the APC/C and, importantly, proteins that contain a short LxCxE motif such as cyclin D, histone deacetylases and chromatin remodelling complexes [146,147,151,153–157] (Figs 2E and 4B). The RB-N regulates the protein–protein interaction capabilities of the pocket domain upon phosphorylation [105,150]. The RB-C domain mediates further interactions with the E2F1-DP1 heterodimer (Fig. 4B). Furthermore, RB proteins recruit the CDK4/6-cyclin D kinase at G1-phase via an RxLxF motif and a distinct C-terminal helix [157,158]. It is estimated that a third of the RB protein sequence lacks stable secondary structure elements. Several disordered segments of RB are targeted by CDK-cyclin-dependent phosphorylation at multiple sites [151]. When RB proteins are hyperphosphorylated, RB-N interacts with the pocket domain thereby masking the LxCxE-binding site and indirectly inactivating the E2F-binding side. This inhibits RB-E2F complex formation and promotes E2F activity on its target genes [105,151,158]. E2F and RB proteins present different affinities for each other: E2F1-E2F3 interact almost exclusively with pRB, whereas E2F4 binds to RBL1 and RBL2 (but also to pRB in some cell types) and E2F5 associates with RBL2 [23,137,159,160]. The RB-E2F complex formation varies throughout the cell cycle. pRb-E2F complexes are most abundant when cells proceed from G1-phase to S-phase, whereas RBL1-E2F complexes are most prevalent in S-phase. RBL2-E2F complexes are present mainly during quiescence and early G1-phase [23,161].

Strikingly, when cells exit the cell cycle and enter quiescence, a massive transcriptional suppression of around 1000 cell cycle-specific genes occurs. This is achieved by the repressive activity of the DREAM (DP, RB-like, E2F and MuvB) complex, which is formed through the association of the RBL2-E2F-DP module with another multiprotein complex, the MuvB (multivulva class B), containing LIN54, LIN9, LIN37, LIN52 and RBBP4 [16,162]. The DREAM complex is recruited to target gene promoters through E2F-DP, which binds to a cell cycle-dependent element (CDE), and LIN54, which binds to the downstream cell cycle genes homology region (CHR) [16,162–165]. Structures of several cell cycle transcription factor DBDs in complex with target DNA sequences have been determined and provide insights into DNA consensus recognition. For example, structures are known for the E2F4-DP2 DBD [166], the E2F8 DBD [167] and the LIN54 DBD [168] (Fig. 4). The interaction between E2F-DP-RBL complex and MuvB is mediated through the smallest subunit LIN52 when phosphorylated by DYRK1A [169]. Biochemical and structural analyses of this interaction revealed that LIN52 binds to the LxCxE cleft of the pocket domain of RBL proteins using the combination of a linear peptide containing a suboptimal LxSxExL sequence and a phosphate at a nearby Ser28 of LIN52 [170] (Figs 2E and 4B). Importantly, the absence of the phosphate-interacting region on the pRb protein explains why MuvB complex specifically assembles with RB-like proteins RBL1-RBL2 and not pRb [170]. The functions of LIN9 and LIN37 are less understood, both functionally and structurally, with initial hints pointing towards LIN9 being a structural component essential for DREAM complex formation, and LIN37 being actively required for gene repression [164,171,172]. RBBP4 is a subunit shared among several chromatin-regulating complexes, and it has been proposed to mediate the interactions between DREAM and chromatin [173,174] (Fig. 4B).

Recent studies have established the key role of the DREAM complex as a master regulator of cell cycle-dependent gene expression and have shown that perturbations in DREAM complex formation are frequently observed in cancers [16,175]. Despite the importance of the DREAM complex, its precise molecular function remains unclear. Unlike chromatin remodelling complexes, the eight-subunit DREAM complex lacks any obvious catalytic subunits posing the question of how it exactly enforces transcriptional repression. Currently, there are two proposed models

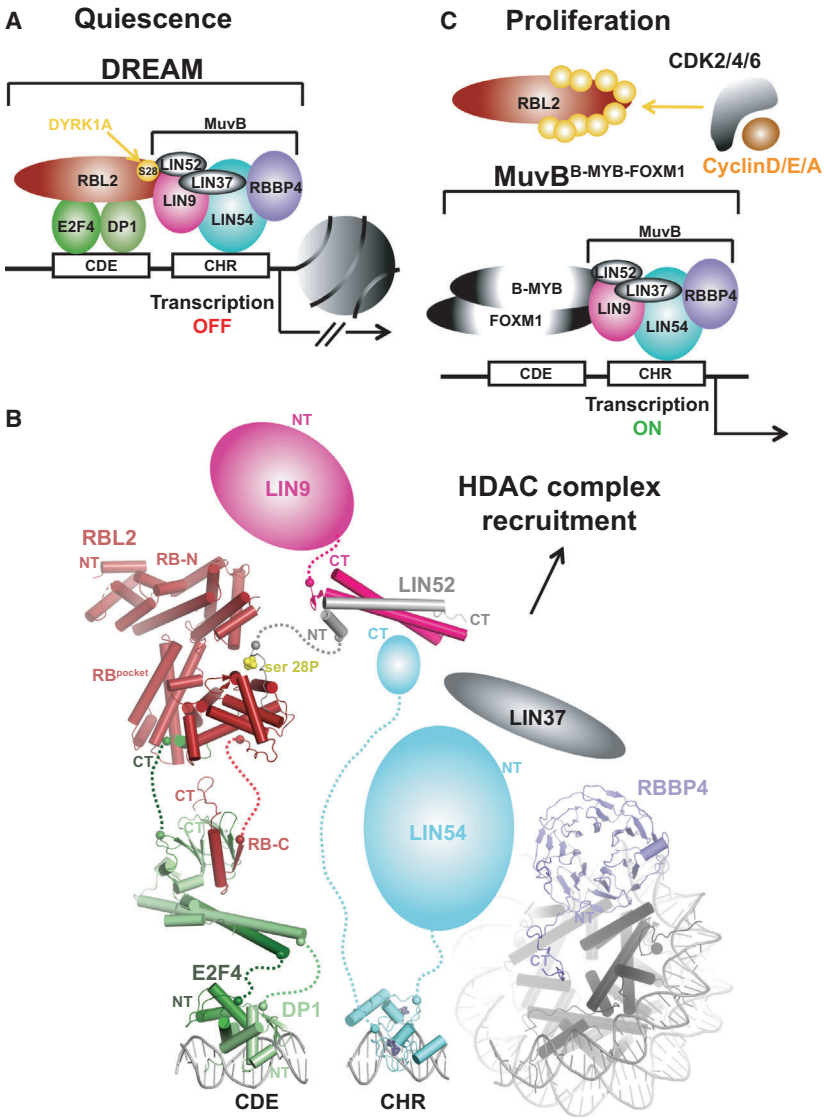

Fig. 4. Transcriptional control of the cell cycle. (A) Schematic cartoon illustrating the subunit composition of the DREAM complex operating in quiescence. The DYRK1 kinase phosphorylates LIN52 at serine 28, which stimulates RBL2-E2F4-DP1 binding to the MuvB complex and DREAM assembly. MuvB consists of LIN54, LIN9, LIN37, LIN52 and RBBP4 subunits. The DREAM complex is a global repressor of cell cycle-dependent transcription. DREAM is targeted to the cell cycle gene promoters via recognition of the CDE by E2F-DP and of the cell CHR by LIN54. (B) The schematic overview in (A) is complemented with a gallery of structures available (PDB IDs: 1CF7, 2AZE, 1N4M, 4YOS, 6C48, 5FD3 and 6KIX). Domains of unknown structure are shown schematically. RB pocket and RB N-terminal domains are represented in red. Serine 28 from LIN52 is shown in yellow. The coiled-coil domain of LIN9, which binds to LIN52 C terminus (grey), is shown in pink. The intrinsically disordered C-terminal domain of RB binds to E2F-DP heterodimer C-terminal domains (green). The N-terminal DBDs of the E2F-DP recognises the CDE element. The CHR element is recognised by LIN54 (light blue). RBBP4 WD40 domain (violet) recognising a nucleosome (grey) is also shown. The mechanism of DREAM-mediated gene repression may involve the recruitment of HDAC complexes. (C) Schematics of events leading to DREAM complex disassembly and formation of $MuvB^{B\text{-}MYB\text{-}FOXM1}$ complex, which activates transcription of cell cycle genes in proliferating cells. CDK-cyclin-dependant phosphorylation of RBL causes the dissociation of MuvB from the RBL-E2F-DP complex. During cell cycle entry, MuvB associates sequentially with B-MYB and FOXM1 transcription factors, which is required for converting MuvB from a transcriptional repressor to an activator. To achieve full transcriptional activation, B-MYB is ubiquitinated by SCF and degraded, and FOXM1 is phosphorylated by Plk1.

of action for the DREAM complex. In the first, the DREAM complex acts as a bridging factor to recruit protein complexes with enzymatic activity. In support of this model, the DREAM complex was shown to interact with Sin3B, a scaffolding protein interacting with HDAC1 (histone deacetylase 1) that has well-established roles in chromatin compaction and subsequent gene repression [120]. In the second model, the DREAM complex could participate in nucleosome assembly and positioning at gene bodies, a process that can occlude RNA polymerase binding and transcription initiation [176].

Another unanswered question is how the same MuvB complex can switch from a quiescence-specific repressor to an activator during cell proliferation. This process involves the dissociation of RB-like proteins from MuvB, which requires the CDK-cyclin-dependent phosphorylation of RBL proteins upon cell cycle entry [161] (Fig. 4A,C). Furthermore, during S-phase, MuvB binds to the B-MYB transcription factor and reassociates with the promoters of a subset of DREAM target genes including mitotic genes [165,177]. Binding of B-MYB to MuvB stimulates recruitment of FOXM1 [177,178]. In late S-phase, B-MYB is phosphorylated by CDK2-cyclin A kinase, which leads to B-MYB ubiquitination by the SCF-Skp2 E3 ligase and proteasomal degradation. Furthermore, FOXM1 is phosphorylated by Plk1. The latter events stimulate the MuvB-FOXM1-dependant transcriptional activation of genes required in the G2/M-phase [179–182]. To date, it is not understood how B-MYB mediates the recruitment of FOXM1 onto the MuvB complex, but also why B-MYB needs to be degraded for transcriptional activation [177,178]. The crystal structure of the domains mediating the MuvB-B-MYB interaction revealed a coiled-coil interaction between LIN9 and LIN52 and a B-MYB helix-turn-helix peptide that binds across this coiled-coil interface [172]. Importantly, this structure shows that the RBL2 and the B-MYB-binding sites on LIN52 do not overlap, pointing to a more complex mechanism of MuvB complex switching from a transcription repressor to an activator [170,172].

In summary, the mechanistic role of MuvB and the precise function of its complexes in regulating cell cycle-dependant transcription remain largely unresolved. Structural studies by X-ray crystallography have been limited to isolated modules of this complex system, as many of these proteins have significant regions of disorder. We envision that cryo-EM has great potential to help in deciphering the structures and the dynamics of these complexes, and in establishing structure–function links that will elucidate their precise mechanism of action. In fact, related chromatin-associated protein complexes have been successfully resolved by cryo-EM as reviewed in Ref. [183]. Among these complexes, we highlight the polycomb repressive complex 2 [184–186], the mixed lineage leukaemia complex [187–189] and the nucleosome remodelling and deacetylase complex [190]. Intriguingly, all these complexes share the RBBP4 core subunit with the MuvB complex, and therefore, it is tempting to think that some of the mechanisms of assembly and chromatin engagement may be conserved among all of these complexes.

Conclusion

The eukaryotic cell cycle is a complex process, which is central to the basic biology of multicellular organisms, and its misregulation lies at the root of several human diseases including cancer. At the heart of this process, the biological oscillator system of the CDK-cyclin kinases is controlled at both the gene level and the protein level by transcription factors and E3 ubiquitin ligases, respectively. During the last decades, high-resolution structural studies on this system have largely relied on X-ray crystallography and NMR to reveal intricate details about the key proteins controlling the cell cycle proteome, actively contributing to our current understanding of different cell cycle events. With cryo-EM now being an integral part of the structural biology toolkit, it is possible to explore these proteins as part of larger assemblies and gain insights into their dynamic nature required for biological activity. Due to the latest advances in both hardware and software, the ‘fuzzy’ picture of these nanomachines has started to clear up, revealing new high-resolution structures and offering new avenues for structure-based drug design.

Nevertheless, single-particle cryo-EM is still limited by the intrinsic flexibility within the protein assemblies. Therefore, X-ray crystallography, NMR and other complementary methods including cross-linking mass spectrometry studies converge together with single-particle cryo-EM in an integrative structural biology effort [191–193]. In addition, tools that allow visualisation of these complexes in their native cellular environment under near-physiological conditions are also emerging very rapidly. Cryo-electron tomography (cryo-TEM) and correlative light and electron microscopy techniques are providing an exciting new era for structural biology [194–197]. Ultimately, time-resolved structural studies on cell cycle regulators will be essential to investigate intermediates of reaction, assembly and remodelling involving these systems [198–200].

Acknowledgements

MGK and CA are supported by the Sir Henry Dale Fellowship 215458/Z/19/Z. We thank Basil J. Greber for discussions.

Conflict of interest

The authors declare no conflict of interest.

Author contributions

MGK and CA conceived the manuscript and wrote the text. CA made the manuscript figures.

References

1 Umbreit NT, Zhang CZ, Lynch LD, Blaine LJ, Cheng AM, Tourdot R, Sun L, Almubarak HF, Judge K, Mitchell TJ *et al*. (2020) Mechanisms generating cancer genome complexity from a single cell division error. *Science* **368**, 282–295.
2 Nelson L, Tighe A, Golder A, Littler S, Bakker B, Moralli D, Murtuza Baker S, Donaldson IJ, Spierings DCJ, Wardenaar R *et al*. (2020) A living biobank of ovarian cancer ex vivo models reveals profound mitotic heterogeneity. *Nat Commun* **11**, 822.
3 Santaguida S & Amon A (2015) Short- and long-term effects of chromosome mis-segregation and aneuploidy. *Nat Rev Mol Cell Biol* **16**, 473–485.
4 Stallaert W, Kedziora KM, Chao HX & Purvis JE (2019) Bistable switches as integrators and actuators during cell cycle progression. *FEBS Lett* **593**, 2805–2816.
5 Novak B & Tyson JJ (2021) Mechanisms of signalling-memory governing progression through the eukaryotic cell cycle. *Curr Opin Cell Biol* **69**, 7–16.
6 Meijer L, Arion D, Golsteyn R, Pines J, Brizuela L, Hunt T & Beach D (1989) Cyclin is a component of the sea urchin egg M-phase specific histone H1 kinase. *EMBO J* **8**, 2275–2282.
7 Simanis V & Nurse P (1986) The cell cycle control gene cdc2+ of fission yeast encodes a protein kinase potentially regulated by phosphorylation. *Cell* **45**, 261–268.
8 Glotzer M, Murray AW & Kirschner MW (1991) Cyclin is degraded by the ubiquitin pathway. *Nature* **349**, 132–138.
9 Goebl MG, Yochem J, Jentsch S, McGrath JP, Varshavsky A & Byers B (1988) The yeast cell cycle gene CDC34 encodes a ubiquitin-conjugating enzyme. *Science* **241**, 1331–1335.
10 Deshaies RJ (1999) SCF and Cullin/Ring H2-based ubiquitin ligases. *Annu Rev Cell Dev Biol* **15**, 435–467.
11 Zachariae W, Shin TH, Galova M, Obermaier B & Nasmyth K (1996) Identification of subunits of the anaphase-promoting complex of Saccharomyces cerevisiae. *Science* **274**, 1201–1204.
12 Hershko A (2010) From rabbit reticulocytes to clam oocytes: in search of the system that targets mitotic cyclins for degradation. *Mol Biol Cell* **21**, 1645–1647.
13 Jang SM, Redon CE, Thakur BL, Bahta MK & Aladjem MI (2020) Regulation of cell cycle drivers by Cullin-RING ubiquitin ligases. *Exp Mol Med* **52**, 1637–1651.
14 Zhang S, Shen Y, Li H, Bi C, Sun Y, Xiong X, Wei W & Sun Y (2020) The negative cross-talk between SAG/RBX2/ROC2 and APC/C E3 Ligases in regulation of cell cycle progression and drug resistance. *Cell Rep* **32**, 108102.
15 Zheng N & Shabek N (2017) Ubiquitin ligases: structure, function, and regulation. *Annu Rev Biochem* **86**, 129–157.
16 Fischer M & Muller GA (2017) Cell cycle transcription control: DREAM/MuvB and RB-E2F complexes. *Crit Rev Biochem Mol Biol* **52**, 638–662.
17 Lanz MC, Dibitetto D & Smolka MB (2019) DNA damage kinase signaling: checkpoint and repair at 30 years. *EMBO J* **38**, e101801.
18 Musacchio A (2015) The molecular biology of spindle assembly checkpoint signaling dynamics. *Curr Biol* **25**, R1002–R1018.
19 Tyson JJ & Novak B (2015) Models in biology: lessons from modeling regulation of the eukaryotic cell cycle. *BMC Biol* **13**, 46.
20 Marescal O & Cheeseman IM (2020) Cellular mechanisms and regulation of quiescence. *Dev Cell* **55**, 259–271.
21 Rubin SM, Sage J & Skotheim JM (2020) Integrating old and new paradigms of G1/S control. *Mol Cell* **80**, 183–192.
22 Pennycook BR & Barr AR (2020) Restriction point regulation at the crossroads between quiescence and cell proliferation. *FEBS Lett* **594**, 2046–2060.
23 Bertoli C, Skotheim JM & de Bruin RAM (2013) Control of cell cycle transcription during G1 and S phases. *Nat Rev Mol Cell Biol* **14**, 518–528.
24 Limas JC & Cook JG (2019) Preparation for DNA replication: the key to a successful S phase. *FEBS Lett* **593**, 2853–2867.
25 Hegarat N, Crncec A, Suarez Peredo Rodriguez MF, Echegaray Iturra F, Gu Y, Busby O, Lang PF, Barr AR, Bakal C, Kanemaki MT *et al*. (2020) Cyclin A triggers Mitosis either via the Greatwall kinase pathway or Cyclin B. *EMBO J* **39**, e104419.
26 Engeland K (2018) Cell cycle arrest through indirect transcriptional repression by p53: I have a DREAM. *Cell Death Differ* **25**, 114–132.
27 Chao WC, Kulkarni K, Zhang Z, Kong EH & Barford D (2012) Structure of the mitotic checkpoint complex. *Nature* **484**, 208–213.

28 Sudakin V, Chan GK & Yen TJ (2001) Checkpoint inhibition of the APC/C in HeLa cells is mediated by a complex of BUBR1, BUB3, CDC20, and MAD2. *J Cell Biol* **154**, 925–936.
29 Primorac I & Musacchio A (2013) Panta rhei: the APC/C at steady state. *J Cell Biol* **201**, 177–189.
30 Clute P & Pines J (1999) Temporal and spatial control of cyclin B1 destruction in metaphase. *Nat Cell Biol* **1**, 82–87.
31 Cohen-Fix O, Peters JM, Kirschner MW & Koshland D (1996) Anaphase initiation in Saccharomyces cerevisiae is controlled by the APC-dependent degradation of the anaphase inhibitor Pds1p. *Genes Dev* **10**, 3081–3093.
32 Uhlmann F, Wernic D, Poupart MA, Koonin EV & Nasmyth K (2000) Cleavage of cohesin by the CD clan protease separin triggers anaphase in yeast. *Cell* **103**, 375–386.
33 Nasmyth K (2002) Segregating sister genomes: the molecular biology of chromosome separation. *Science* **297**, 559–565.
34 Foster SA & Morgan DO (2012) The APC/C subunit Mnd2/Apc15 promotes Cdc20 autoubiquitination and spindle assembly checkpoint inactivation. *Mol Cell* **47**, 921–932.
35 Uzunova K, Dye BT, Schutz H, Ladurner R, Petzold G, Toyoda Y, Jarvis MA, Brown NG, Poser I, Novatchkova M *et al*. (2012) APC15 mediates CDC20 autoubiquitylation by APC/C(MCC) and disassembly of the mitotic checkpoint complex. *Nat Struct Mol Biol* **19**, 1116–1123.
36 Mansfeld J, Collin P, Collins MO, Choudhary JS & Pines J (2011) APC15 drives the turnover of MCC-CDC20 to make the spindle assembly checkpoint responsive to kinetochore attachment. *Nat Cell Biol* **13**, 1234–1243.
37 Collin P, Nashchekina O, Walker R & Pines J (2013) The spindle assembly checkpoint works like a rheostat rather than a toggle switch. *Nat Cell Biol* **15**, 1378–1385.
38 Chen C, Whitney IP, Banerjee A, Sacristan C, Sekhri P, Kern DM, Fontan A, Kops G, Tyson JJ, Cheeseman IM *et al*. (2019) Ectopic activation of the spindle assembly checkpoint signaling cascade reveals its biochemical design. *Curr Biol* **29**, 104–119.e10.
39 Alfieri C, Zhang S & Barford D (2017) Visualizing the complex functions and mechanisms of the anaphase promoting complex/cyclosome (APC/C). *Open Biol* **7**, 1–27.
40 Watson ER, Brown NG, Peters JM, Stark H & Schulman BA (2019) Posing the APC/C E3 ubiquitin ligase to orchestrate cell division. *Trends Cell Biol* **29**, 117–134.
41 Barford D (2020) Structural interconversions of the anaphase-promoting complex/cyclosome (APC/C) regulate cell cycle transitions. *Curr Opin Struct Biol* **61**, 86–97.
42 Eastman AE & Guo S (2020) The palette of techniques for cell cycle analysis. *FEBS Lett* **594**, 2084–2098.
43 Wang HW & Wang JW (2017) How cryo-electron microscopy and X-ray crystallography complement each other. *Protein Sci* **26**, 32–39.
44 Shi Y (2014) A glimpse of structural biology through X-ray crystallography. *Cell* **159**, 995–1014.
45 Gauto DF, Estrozi LF, Schwieters CD, Effantin G, Macek P, Sounier R, Sivertsen AC, Schmidt E, Kerfah R, Mas G *et al*. (2019) Integrated NMR and cryo-EM atomic-resolution structure determination of a half-megadalton enzyme complex. *Nat Commun* **10**, 2697.
46 Davey NE & Morgan DO (2016) Building a regulatory network with short linear sequence motifs: lessons from the degrons of the anaphase-promoting complex. *Mol Cell* **64**, 12–23.
47 Cheng Y (2018) Single-particle cryo-EM-How did it get here and where will it go. *Science* **361**, 876–880.
48 Nakane T, Kotecha A, Sente A, McMullan G, Masiulis S, Brown P, Grigoras IT, Malinauskaite L, Malinauskas T, Miehling J *et al*. (2020) Single-particle cryo-EM at atomic resolution. *Nature* **587**, 152–156.
49 Fernandez-Leiro R & Scheres SH (2016) Unravelling biological macromolecules with cryo-electron microscopy. *Nature* **537**, 339–346.
50 Cheng Y, Grigorieff N, Penczek PA & Walz T (2015) A primer to single-particle cryo-electron microscopy. *Cell* **161**, 438–449.
51 Malumbres M & Barbacid M (2005) Mammalian cyclin-dependent kinases. *Trends Biochem Sci* **30**, 630–641.
52 Loyer P & Trembley JH (2020) Roles of CDK/Cyclin complexes in transcription and pre-mRNA splicing: Cyclins L and CDK11 at the cross-roads of cell cycle and regulation of gene expression. *Semin Cell Dev Biol* **107**, 36–45.
53 Shi Y (2009) Serine/threonine phosphatases: mechanism through structure. *Cell* **139**, 468–484.
54 Wood DJ & Endicott JA (2018) Structural insights into the functional diversity of the CDK–cyclin family. *Open Biol* **8**, 180112.
55 Schulze-Gahmen U, De Bondt HL & Kim SH (1996) High-resolution crystal structures of human cyclin-dependent kinase 2 with and without ATP: bound waters and natural ligand as guides for inhibitor design. *J Med Chem* **39**, 4540–4546.
56 Jeffrey PD, Russo AA, Polyak K, Gibbs E, Hurwitz J, Massague J & Pavletich NP (1995) Mechanism of CDK activation revealed by the structure of a cyclinA-CDK2 complex. *Nature* **376**, 313–320.
57 Russo AA, Jeffrey PD & Pavletich NP (1996) Structural basis of cyclin-dependent kinase activation by phosphorylation. *Nat Struct Biol* **3**, 696–700.
58 Brown NR, Korolchuk S, Martin MP, Stanley WA, Moukhametzianov R, Noble MEM & Endicott JA

(2015) CDK1 structures reveal conserved and unique features of the essential cell cycle CDK. *Nat Commun* **6**, 6769.
59 Guiley KZ, Stevenson JW, Lou K, Barkovich KJ, Kumarasamy V, Wijeratne TU, Bunch KL, Tripathi S, Knudsen ES, Witkiewicz AK *et al.* (2019) p27 allosterically activates cyclin-dependent kinase 4 and antagonizes palbociclib inhibition. *Science* **366**, eaaw2106.
60 Noble ME, Endicott JA, Brown NR & Johnson LN (1997) The cyclin box fold: protein recognition in cell-cycle and transcription control. *Trends Biochem Sci* **22**, 482–487.
61 Takeda DY, Wohlschlegel JA & Dutta A (2001) A bipartite substrate recognition motif for cyclin-dependent kinases. *J Biol Chem* **276**, 1993–1997.
62 Ord M, Venta R, Moll K, Valk E & Loog M (2019) Cyclin-specific docking mechanisms reveal the complexity of M-CDK function in the cell cycle. *Mol Cell* **75**, 76–89.e3.
63 Koivomagi M, Ord M, Iofik A, Valk E, Venta R, Faustova I, Kivi R, Balog ER, Rubin SM & Loog M (2013) Multisite phosphorylation networks as signal processors for Cdk1. *Nat Struct Mol Biol* **20**, 1415–1424.
64 McGrath DA, Balog ER, Koivomagi M, Lucena R, Mai MV, Hirschi A, Kellogg DR, Loog M & Rubin SM (2013) Cks confers specificity to phosphorylation-dependent CDK signaling pathways. *Nat Struct Mol Biol* **20**, 1407–1414.
65 Venta R, Valk E, Ord M, Kosik O, Paabo K, Maljavin A, Kivi R, Faustova I, Shtaida N, Lepiku M *et al.* (2020) A processive phosphorylation circuit with multiple kinase inputs and mutually diversional routes controls G1/S decision. *Nat Commun* **11**, 1836.
66 Ord M, Moll K, Agerova A, Kivi R, Faustova I, Venta R, Valk E & Loog M (2019) Multisite phosphorylation code of CDK. *Nat Struct Mol Biol* **26**, 649–658.
67 Russo AA, Jeffrey PD, Patten AK, Massague J & Pavletich NP (1996) Crystal structure of the p27Kip1 cyclin-dependent-kinase inhibitor bound to the cyclin A-Cdk2 complex. *Nature* **382**, 325–331.
68 Oki T, Nishimura K, Kitaura J, Togami K, Maehara A, Izawa K, Sakaue-Sawano A, Niida A, Miyano S, Aburatani H *et al.* (2014) A novel cell-cycle-indicator, mVenus-p27K-, identifies quiescent cells and visualizes G0–G1 transition. *Sci Rep* **4**, 4012.
69 Barr AR, Cooper S, Heldt FS, Butera F, Stoy H, Mansfeld J, Novak B & Bakal C (2017) DNA damage during S-phase mediates the proliferation-quiescence decision in the subsequent G1 via p21 expression. *Nat Commun* **8**, 14728.
70 Day PJ, Cleasby A, Tickle IJ, O'Reilly M, Coyle JE, Holding FP, McMenamin RL, Yon J, Chopra R, Lengauer C *et al.* (2009) Crystal structure of human CDK4 in complex with a D-type cyclin. *Proc Natl Acad Sci USA* **106**, 4166–4170.
71 Takaki T, Echalier A, Brown NR, Hunt T, Endicott JA & Noble ME (2009) The structure of CDK4/cyclin D3 has implications for models of CDK activation. *Proc Natl Acad Sci USA* **106**, 4171–4176.
72 Greber BJ, Perez-Bertoldi JM, Lim K, Iavarone AT, Toso DB & Nogales E (2020) The cryoelectron microscopy structure of the human CDK-activating kinase. *Proc Natl Acad Sci USA* **117**, 22849–22857.
73 Greber BJ, Remis J, Ali S & Nogales E (2021) 2.5A-resolution structure of the human CDK-activating kinase bound to the clinical inhibitor ICEC0942. *Biophys J* **120**, 677–686.
74 Asghar U, Witkiewicz AK, Turner NC & Knudsen ES (2015) The history and future of targeting cyclin-dependent kinases in cancer therapy. *Nat Rev Drug Discov* **14**, 130–146.
75 Wells CI, Vasta JD, Corona CR, Wilkinson J, Zimprich CA, Ingold MR, Pickett JE, Drewry DH, Pugh KM, Schwinn MK *et al.* (2020) Quantifying CDK inhibitor selectivity in live cells. *Nat Commun* **11**, 2743.
76 Ding L, Cao J, Lin W, Chen H, Xiong X, Ao H, Yu M, Lin J & Cui Q. (2020) The roles of cyclin-dependent kinases in cell-cycle progression and therapeutic strategies in human breast cancer. *Int J Mol Sci* **21**, 1960.
77 Verba KA, Wang RY, Arakawa A, Liu Y, Shirouzu M, Yokoyama S & Agard DA (2016) Atomic structure of Hsp90-Cdc37-Cdk4 reveals that Hsp90 traps and stabilizes an unfolded kinase. *Science* **352**, 1542–1547.
78 Teixeira LK & Reed SI (2013) Ubiquitin ligases and cell cycle control. *Annu Rev Biochem* **82**, 387–414.
79 Soucy TA, Smith PG, Milhollen MA, Berger AJ, Gavin JM, Adhikari S, Brownell JE, Burke KE, Cardin DP, Critchley S *et al.* (2009) An inhibitor of NEDD8-activating enzyme as a new approach to treat cancer. *Nature* **458**, 732–736.
80 Willems AR, Schwab M & Tyers M (2004) A hitchhiker's guide to the cullin ubiquitin ligases: SCF and its kin. *Biochim Biophys Acta* **1695**, 133–170.
81 Cardozo T & Pagano M (2004) The SCF ubiquitin ligase: insights into a molecular machine. *Nat Rev Mol Cell Biol* **5**, 739–751.
82 Zheng N, Schulman BA, Song L, Miller JJ, Jeffrey PD, Wang P, Chu C, Koepp DM, Elledge SJ, Pagano M *et al.* (2002) Structure of the Cul1-Rbx1-Skp1-F boxSkp2 SCF ubiquitin ligase complex. *Nature* **416**, 703–709.
83 Duda DM, Borg LA, Scott DC, Hunt HW, Hammel M & Schulman BA (2008) Structural insights into NEDD8 activation of cullin-RING ligases: conformational control of conjugation. *Cell* **134**, 995–1006.

84 Goldenberg SJ, Cascio TC, Shumway SD, Garbutt KC, Liu J, Xiong Y & Zheng N (2004) Structure of the Cand1-Cul1-Roc1 complex reveals regulatory mechanisms for the assembly of the multisubunit cullin-dependent ubiquitin ligases. *Cell* **119**, 517–528.
85 Pan ZQ, Kentsis A, Dias DC, Yamoah K & Wu K (2004) Nedd8 on cullin: building an expressway to protein destruction. *Oncogene* **23**, 1985–1997.
86 Saha A & Deshaies RJ (2008) Multimodal activation of the ubiquitin ligase SCF by Nedd8 conjugation. *Mol Cell* **32**, 21–31.
87 Baek K, Krist DT, Prabu JR, Hill S, Klugel M, Neumaier LM, von Gronau S, Kleiger G & Schulman BA (2020) NEDD8 nucleates a multivalent cullin-RING-UBE2D ubiquitin ligation assembly. *Nature* **578**, 461–466.
88 Baek K, Scott DC & Schulman BA (2020) NEDD8 and ubiquitin ligation by cullin-RING E3 ligases. *Curr Opin Struct Biol* **67**, 101–109.
89 Mosadeghi R, Reichermeier KM, Winkler M, Schreiber A, Reitsma JM, Zhang Y, Stengel F, Cao J, Kim M, Sweredoski MJ *et al.* (2016) Structural and kinetic analysis of the COP9-Signalosome activation and the cullin-RING ubiquitin ligase deneddylation cycle. *Elife* **5**, 1–25.
90 Faull SV, Lau AMC, Martens C, Ahdash Z, Hansen K, Yebenes H, Schmidt C, Beuron F, Cronin NB, Morris EP *et al.* (2019) Structural basis of Cullin 2 RING E3 ligase regulation by the COP9 signalosome. *Nat Commun* **10**, 3814.
91 Jin J, Cardozo T, Lovering RC, Elledge SJ, Pagano M & Harper JW (2004) Systematic analysis and nomenclature of mammalian F-box proteins. *Genes Dev* **18**, 2573–2580.
92 Skaar JR, Pagan JK & Pagano M (2013) Mechanisms and function of substrate recruitment by F-box proteins. *Nat Rev Mol Cell Biol* **14**, 369–381.
93 Bai C, Richman R & Elledge SJ (1994) Human cyclin F. *EMBO J* **13**, 6087–6098.
94 Bai C, Sen P, Hofmann K, Ma L, Goebl M, Harper JW & Elledge SJ (1996) SKP1 connects cell cycle regulators to the ubiquitin proteolysis machinery through a novel motif, the F-box. *Cell* **86**, 263–274.
95 D'Angiolella V, Esencay M & Pagano M (2013) A cyclin without cyclin-dependent kinases: cyclin F controls genome stability through ubiquitin-mediated proteolysis. *Trends Cell Biol* **23**, 135–140.
96 Choudhury R, Bonacci T, Arceci A, Lahiri D, Mills CA, Kernan JL, Branigan TB, DeCaprio JA, Burke DJ & Emanuele MJ (2016) APC/C and SCF(cyclin F) constitute a reciprocal feedback circuit controlling S-phase entry. *Cell Rep* **16**, 3359–3372.
97 Frescas D & Pagano M (2008) Deregulated proteolysis by the F-box proteins SKP2 and beta-TrCP: tipping the scales of cancer. *Nat Rev Cancer* **8**, 438–449.
98 Pagano M, Tam SW, Theodoras AM, Beer-Romero P, Del Sal G, Chau V, Yew PR, Draetta GF & Rolfe M (1995) Role of the ubiquitin-proteasome pathway in regulating abundance of the cyclin-dependent kinase inhibitor p27. *Science* **269**, 682–685.
99 Carrano AC, Eytan E, Hershko A & Pagano M (1999) SKP2 is required for ubiquitin-mediated degradation of the CDK inhibitor p27. *Nat Cell Biol* **1**, 193–199.
100 Montagnoli A, Fiore F, Eytan E, Carrano AC, Draetta GF, Hershko A & Pagano M (1999) Ubiquitination of p27 is regulated by Cdk-dependent phosphorylation and trimeric complex formation. *Gene Dev* **13**, 1181–1189.
101 Hao B, Zheng N, Schulman BA, Wu G, Miller JJ, Pagano M & Pavletich NP (2005) Structural basis of the Cks1-dependent recognition of p27(Kip1) by the SCF(Skp2) ubiquitin ligase. *Mol Cell* **20**, 9–19.
102 Cobrinik D (2005) Pocket proteins and cell cycle control. *Oncogene* **24**, 2796–2809.
103 Tedesco D, Lukas J & Reed SI (2002) The pRb-related protein p130 is regulated by phosphorylation-dependent proteolysis via the protein-ubiquitin ligase SCF(Skp2). *Genes Dev* **16**, 2946–2957.
104 Bhattacharya S, Garriga J, Calbo J, Yong T, Haines DS & Grana X (2003) SKP2 associates with p130 and accelerates p130 ubiquitylation and degradation in human cells. *Oncogene* **22**, 2443–2451.
105 Burke JR, Hura GL & Rubin SM (2012) Structures of inactive retinoblastoma protein reveal multiple mechanisms for cell cycle control. *Genes Dev* **26**, 1156–1166.
106 Strohmaier H, Spruck CH, Kaiser P, Won KA, Sangfelt O & Reed SI (2001) Human F-box protein hCdc4 targets cyclin E for proteolysis and is mutated in a breast cancer cell line. *Nature* **413**, 316–322.
107 Welcker M, Singer J, Loeb KR, Grim J, Bloecher A, Gurien-West M, Clurman BE & Roberts JM (2003) Multisite phosphorylation by Cdk2 and GSK3 controls cyclin E degradation. *Mol Cell* **12**, 381–392.
108 Hao B, Oehlmann S, Sowa ME, Harper JW & Pavletich NP (2007) Structure of a Fbw7-Skp1-cyclin E complex: multisite-phosphorylated substrate recognition by SCF ubiquitin ligases. *Mol Cell* **26**, 131–143.
109 Horn-Ghetko D, Krist DT, Prabu JR, Baek K, Mulder MPC, Klugel M, Scott DC, Ovaa H, Kleiger G & Schulman BA (2021) Ubiquitin ligation to F-box protein targets by SCF-RBR E3–E3 super-assembly. *Nature* **7847**, 671–676.
110 Scott DC, Rhee DY, Duda DM, Kelsall IR, Olszewski JL, Paulo JA, de Jong A, Ovaa H, Alpi AF, Harper JW *et al.* (2016) Two distinct types of E3 ligases work in unison to regulate substrate ubiquitylation. *Cell* **166**, 1198–1214.e24.

111 Horn-Ghetko D, Krist DT, Prabu JR, Baek K, Mulder MPC, Klugel M, Scott DC, Ovaa H, Kleiger G & Schulman BA (2021) Ubiquitin ligation to F-box protein targets by SCF-RBR E3–E3 super-assembly. *Nature* **590**, 671–676.
112 Li Y, Jin K, Bunker E, Zhang X, Luo X, Liu X & Hao B (2018) Structural basis of the phosphorylation-independent recognition of cyclin D1 by the SCF (FBXO31) ubiquitin ligase. *Proc Natl Acad Sci USA* **115**, 319–324.
113 Li Y & Hao B (2010) Structural basis of dimerization-dependent ubiquitination by the SCF(Fbx4) ubiquitin ligase. *J Biol Chem* **285**, 13896–13906.
114 Yumimoto K, Yamauchi Y & Nakayama KI (2020) F-box proteins and cancer. *Cancers (Basel)* **12**, 1249.
115 Bulatov E & Ciulli A (2015) Targeting Cullin-RING E3 ubiquitin ligases for drug discovery: structure, assembly and small-molecule modulation. *Biochem J* **467**, 365–386.
116 Barford D (2011) Structural insights into anaphase-promoting complex function and mechanism. *Philos Trans R Soc Lond B Biol Sci* **366**, 3605–3624.
117 Chang L, Zhang Z, Yang J, McLaughlin SH & Barford D (2015) Atomic structure of the APC/C and its mechanism of protein ubiquitination. *Nature* **522**, 450–454.
118 Visintin R, Prinz S & Amon A (1997) CDC20 and CDH1: a family of substrate-specific activators of APC-dependent proteolysis. *Science* **278**, 460–463.
119 Sivakumar S & Gorbsky GJ (2015) Spatiotemporal regulation of the anaphase-promoting complex in mitosis. *Nat Rev Mol Cell Biol* **16**, 82–94.
120 Bainor AJ, Saini S, Calderon A, Casado-Polanco R, Giner-Ramirez B, Moncada C, Cantor DJ, Ernlund A, Litovchick L & David G (2018) The HDAC-associated Sin3B protein represses DREAM complex targets and cooperates with APC/C to promote quiescence. *Cell Rep* **25**, 2797–2807.e8.
121 Cappell SD, Mark KG, Garbett D, Pack LR, Rape M & Meyer T (2018) EMI1 switches from being a substrate to an inhibitor of APC/C(CDH1) to start the cell cycle. *Nature* **558**, 313–317.
122 Pfleger CM & Kirschner MW (2000) The KEN box: an APC recognition signal distinct from the D box targeted by Cdh1. *Genes Dev* **14**, 655–665.
123 Di Fiore B, Davey NE, Hagting A, Izawa D, Mansfeld J, Gibson TJ & Pines J (2015) The ABBA motif binds APC/C activators and is shared by APC/C substrates and regulators. *Dev Cell* **32**, 358–372.
124 He J, Chao WC, Zhang Z, Yang J, Cronin N & Barford D (2013) Insights into degron recognition by APC/C coactivators from the structure of an Acm1-Cdh1 complex. *Mol Cell* **50**, 649–660.
125 da Fonseca PC, Kong EH, Zhang Z, Schreiber A, Williams MA, Morris EP & Barford D (2011) Structures of APC/C(Cdh1) with substrates identify Cdh1 and Apc10 as the D-box co-receptor. *Nature* **470**, 274–278.
126 Hayes MJ, Kimata Y, Wattam SL, Lindon C, Mao G, Yamano H & Fry AM (2006) Early mitotic degradation of Nek2A depends on Cdc20-independent interaction with the APC/C. *Nat Cell Biol* **8**, 607–614.
127 Boekhout M & Wolthuis R (2015) Nek2A destruction marks APC/C activation at the prophase-to-prometaphase transition by spindle-checkpoint-restricted Cdc20. *J Cell Sci* **128**, 1639–1653.
128 Alfieri C, Tischer T & Barford D (2020) A unique binding mode of Nek2A to the APC/C allows its ubiquitination during prometaphase. *EMBO Rep* **21**, e49831.
129 Sedgwick GG, Hayward DG, Di Fiore B, Pardo M, Yu L, Pines J & Nilsson J (2013) Mechanisms controlling the temporal degradation of Nek2A and Kif18A by the APC/C-Cdc20 complex. *EMBO J* **32**, 303–314.
130 Zhang S, Chang L, Alfieri C, Zhang Z, Yang J, Maslen S, Skehel M & Barford D (2016) Molecular mechanism of APC/C activation by mitotic phosphorylation. *Nature* **533**, 260–264.
131 Alfieri C, Chang L, Zhang Z, Yang J, Maslen S, Skehel M & Barford D (2016) Molecular basis of APC/C regulation by the spindle assembly checkpoint. *Nature* **536**, 431–436.
132 Chang LF, Zhang Z, Yang J, McLaughlin SH & Barford D (2014) Molecular architecture and mechanism of the anaphase-promoting complex. *Nature* **513**, 388–393.
133 Das AK, Cohen PW & Barford D (1998) The structure of the tetratricopeptide repeats of protein phosphatase 5: implications for TPR-mediated protein-protein interactions. *EMBO J* **17**, 1192–1199.
134 Brown NG, VanderLinden R, Watson ER, Qiao R, Grace CR, Yamaguchi M, Weissmann F, Frye JJ, Dube P, Ei Cho S *et al.* (2015) RING E3 mechanism for ubiquitin ligation to a disordered substrate visualized for human anaphase-promoting complex. *Proc Natl Acad Sci USA* **112**, 5272–5279.
135 Yamaguchi M, VanderLinden R, Weissmann F, Qiao R, Dube P, Brown NG, Haselbach D, Zhang W, Sidhu SS, Peters JM *et al.* (2016) Cryo-EM of mitotic checkpoint complex-bound APC/C reveals reciprocal and conformational regulation of ubiquitin ligation. *Mol Cell* **63**, 593–607.
136 Sitry-Shevah D, Kaisari S, Teichner A, Miniowitz-Shemtov S & Hershko A (2018) Role of ubiquitylation of components of mitotic checkpoint complex in their dissociation from anaphase-promoting complex/cyclosome. *Proc Natl Acad Sci USA* **115**, 1777–1782.
137 Kent LN & Leone G (2019) The broken cycle: E2F dysfunction in cancer. *Nat Rev Cancer* **19**, 326–338.

138 Dyson N (1998) The regulation of E2F by pRB-family proteins. *Gene Dev* **12**, 2245–2262.
139 Dimova DK & Dyson NJ (2005) The E2F transcriptional network: old acquaintances with new faces. *Oncogene* **24**, 2810–2826.
140 Cuitino MC, Pecot T, Sun D, Kladney R, Okano-Uchida T, Shinde N, Saeed R, Perez-Castro AJ, Webb A, Liu T *et al*. (2019) Two distinct E2F transcriptional modules drive cell cycles and differentiation. *Cell Rep* **27**, 3547–3560.e5.
141 Emanuele MJ, Enrico TP, Mouery RD, Wasserman D, Nachum S & Tzur A (2020) Complex cartography: regulation of E2F transcription factors by cyclin F and Ubiquitin. *Trends Cell Biol* **30**, 640–652.
142 Burdova K, Yang H, Faedda R, Hume S, Chauhan J, Ebner D, Kessler BM, Vendrell I, Drewry DH, Wells CI *et al*. (2019) E2F1 proteolysis via SCF-cyclin F underlies synthetic lethality between cyclin F loss and Chk1 inhibition. *EMBO J* **38**, e101443.
143 Clijsters L, Hoencamp C, Calis JJA, Marzio A, Handgraaf SM, Cuitino MC, Rosenberg BR, Leone G & Pagano M (2019) Cyclin F controls cell-cycle transcriptional outputs by directing the degradation of the three activator E2Fs. *Mol Cell* **74**, 1264–1277.e7.
144 Boekhout M, Yuan R, Wondergem AP, Segeren HA, van Liere EA, Awol N, Jansen I, Wolthuis RM, de Bruin A & Westendorp B (2016) Feedback regulation between atypical E2Fs and APC/CCdh1 coordinates cell cycle progression. *EMBO Rep* **17**, 414–427.
145 Yuan R, Liu Q, Segeren HA, Yuniati L, Guardavaccaro D, Lebbink RJ, Westendorp B & de Bruin A (2019) Cyclin F-dependent degradation of E2F7 is critical for DNA repair and G2-phase progression. *EMBO J* **38**, e101430.
146 Xiao B, Spencer J, Clements A, Ali-Khan N, Mittnacht S, Broceno C, Burghammer M, Perrakis A, Marmorstein R & Gamblin SJ (2003) Crystal structure of the retinoblastoma tumor suppressor protein bound to E2F and the molecular basis of its regulation. *Proc Natl Acad Sci USA* **100**, 2363–2368.
147 Lee C, Chang JH, Lee HS & Cho Y (2002) Structural basis for the recognition of the E2F transactivation domain by the retinoblastoma tumor suppressor. *Genes Dev* **16**, 3199–3212.
148 Yao G, Lee TJ, Mori S, Nevins JR & You L (2008) A bistable Rb-E2F switch underlies the restriction point. *Nat Cell Biol* **10**, 476–482.
149 Burkhart DL & Sage J (2008) Cellular mechanisms of tumour suppression by the retinoblastoma gene. *Nat Rev Cancer* **8**, 671–682.
150 Hassler M, Singh S, Yue WW, Luczynski M, Lakbir R, Sanchez-Sanchez F, Bader T, Pearl LH & Mittnacht S (2007) Crystal structure of the retinoblastoma protein N domain provides insight into tumor suppression, ligand interaction, and holoprotein architecture. *Mol Cell* **28**, 371–385.
151 Rubin SM (2013) Deciphering the retinoblastoma protein phosphorylation code. *Trends Biochem Sci* **38**, 12–19.
152 Lee JO, Russo AA & Pavletich NP (1998) Structure of the retinoblastoma tumour-suppressor pocket domain bound to a peptide from HPV E7. *Nature* **391**, 859–865.
153 Binne UK, Classon MK, Dick FA, Wei W, Rape M, Kaelin WG Jr, Naar AM & Dyson NJ (2007) Retinoblastoma protein and anaphase-promoting complex physically interact and functionally cooperate during cell-cycle exit. *Nat Cell Biol* **9**, 225–232.
154 Brehm A, Miska EA, McCance DJ, Reid JL, Bannister AJ & Kouzarides T (1998) Retinoblastoma protein recruits histone deacetylase to repress transcription. *Nature* **391**, 597–601.
155 Magnaghi-Jaulin L, Groisman R, Naguibneva I, Robin P, Lorain S, Le Villain JP, Troalen F, Trouche D & Harel-Bellan A (1998) Retinoblastoma protein represses transcription by recruiting a histone deacetylase. *Nature* **391**, 601–605.
156 Uchida C (2016) Roles of pRB in the regulation of nucleosome and chromatin structures. *Biomed Res Int* **2016**, 5959721.
157 Topacio BR, Zatulovskiy E, Cristea S, Xie S, Tambo CS, Rubin SM, Sage J, Koivomagi M & Skotheim JM (2019) Cyclin D-Cdk 4,6 drives cell-cycle progression via the retinoblastoma protein's C-Terminal helix. *Mol Cell* **74**, 758–770.e4.
158 Rubin SM, Gall AL, Zheng N & Pavletich NP (2005) Structure of the Rb C-terminal domain bound to E2F1-DP1: a mechanism for phosphorylation-induced E2F release. *Cell* **123**, 1093–1106.
159 Liban TJ, Medina EM, Tripathi S, Sengupta S, Henry RW, Buchler NE & Rubin SM (2017) Conservation and divergence of C-terminal domain structure in the retinoblastoma protein family. *Proc Natl Acad Sci USA* **114**, 4942–4947.
160 Liban TJ, Thwaites MJ, Dick FA & Rubin SM (2016) Structural conservation and E2F binding specificity within the retinoblastoma pocket protein family. *J Mol Biol* **428**, 3960–3971.
161 Henley SA & Dick FA (2012) The retinoblastoma family of proteins and their regulatory functions in the mammalian cell division cycle. *Cell Div* **7**, 10.
162 Litovchick L, Sadasivam S, Florens L, Zhu X, Swanson SK, Velmurugan S, Chen R, Washburn MP, Liu XS & DeCaprio JA (2007) Evolutionarily conserved multisubunit RBL2/p130 and E2F4 protein complex represses human cell cycle-dependent genes in quiescence. *Mol Cell* **26**, 539–551.
163 Pilkinton M, Sandoval R & Colamonici OR (2007) Mammalian Mip/LIN-9 interacts with either the p107, p130/E2F4 repressor complex or B-Myb in a cell

cycle-phase-dependent context distinct from the *Drosophila* dREAM complex. *Oncogene* **26**, 7535–7543.
164 Schmit F, Korenjak M, Mannefeld M, Schmitt K, Franke C, von Eyss B, Gagrica S, Hanel F, Brehm A & Gaubatz S (2007) LINC, a human complex that is related to pRB-containing complexes in invertebrates regulates the expression of G2/M genes. *Cell Cycle* **6**, 1903–1913.
165 Muller GA, Quaas M, Schumann M, Krause E, Padi M, Fischer M, Litovchick L, DeCaprio JA & Engeland K (2012) The CHR promoter element controls cell cycle-dependent gene transcription and binds the DREAM and MMB complexes. *Nucleic Acids Res* **40**, 1561–1578.
166 Zheng N, Fraenkel E, Pabo CO & Pavletich NP (1999) Structural basis of DNA recognition by the heterodimeric cell cycle transcription factor E2F-DP. *Genes Dev* **13**, 666–674.
167 Morgunova E, Yin Y, Jolma A, Dave K, Schmierer B, Popov A, Eremina N, Nilsson L & Taipale J (2015) Structural insights into the DNA-binding specificity of E2F family transcription factors. *Nat Commun* **6**, 10050.
168 Marceau AH, Felthousen JG, Goetsch PD, Iness AN, Lee HW, Tripathi SM, Strome S, Litovchick L & Rubin SM (2016) Structural basis for LIN54 recognition of CHR elements in cell cycle-regulated promoters. *Nat Commun* **7**, 12301.
169 Litovchick L, Florens LA, Swanson SK, Washburn MP & DeCaprio JA (2011) DYRK1A protein kinase promotes quiescence and senescence through DREAM complex assembly. *Genes Dev* **25**, 801–813.
170 Guiley KZ, Liban TJ, Felthousen JG, Ramanan P, Litovchick L & Rubin SM (2015) Structural mechanisms of DREAM complex assembly and regulation. *Genes Dev* **29**, 961–974.
171 Mages CF, Wintsche A, Bernhart SH & Muller GA (2017) The DREAM complex through its subunit Lin37 cooperates with Rb to initiate quiescence. *Elife* **6**, 1–23.
172 Guiley KZ, Iness AN, Saini S, Tripathi S, Lipsick JS, Litovchick L & Rubin SM (2018) Structural mechanism of Myb-MuvB assembly. *Proc Natl Acad Sci USA* **115**, 10016–10021.
173 Murzina NV, Pei XY, Zhang W, Sparkes M, Vicente-Garcia J, Pratap JV, McLaughlin SH, Ben-Shahar TR, Verreault A, Luisi BF *et al*. (2008) Structural basis for the recognition of histone H4 by the histone-chaperone RbAp46. *Structure* **16**, 1077–1085.
174 Zhang W, Tyl M, Ward R, Sobott F, Maman J, Murthy AS, Watson AA, Fedorov O, Bowman A, Owen-Hughes T *et al*. (2013) Structural plasticity of histones H3–H4 facilitates their allosteric exchange between RbAp48 and ASF1. *Nat Struct Mol Biol* **20**, 29–U43.
175 Sadasivam S & DeCaprio JA (2013) The DREAM complex: master coordinator of cell cycle-dependent gene expression. *Nat Rev Cancer* **13**, 585–595.
176 Latorre I, Chesney MA, Garrigues JM, Stempor P, Appert A, Francesconi M, Strome S & Ahringer J (2015) The DREAM complex promotes gene body H2A.Z for target repression. *Genes Dev* **29**, 495–500.
177 Sadasivam S, Duan S & DeCaprio JA (2012) The MuvB complex sequentially recruits B-Myb and FoxM1 to promote mitotic gene expression. *Genes Dev* **26**, 474–489.
178 Down CF, Millour J, Lam EWF & Watson RJ (2012) Binding of FoxM1 to G2/M gene promoters is dependent upon B-Myb. *BBA-Gene Regul Mech* **1819**, 855–862.
179 Charrasse S, Carena I, Brondani V, Klempnauer KH & Ferrari S (2000) Degradation of B-Myb by ubiquitin-mediated proteolysis: involvement of the Cdc34-SCFp45Skp2 pathway. *Oncogene* **19**, 2986–2995.
180 Ziebold U, Bartsch O, Marais R, Ferrari S & Klempnauer KH (1997) Phosphorylation and activation of B-Myb by cyclin A-Cdk2. *Curr Biol* **7**, 253–260.
181 Saville MK & Watson RJ (1998) The cell-cycle regulated transcription factor B-Myb is phosphorylated by cyclin A/Cdk2 at sites that enhance its transactivation properties. *Oncogene* **17**, 2679–2689.
182 Marceau AH, Brison CM, Nerli S, Arsenault HE, McShan AC, Chen E, Lee HW, Benanti JA, Sgourakis NG & Rubin SM (2019) An order-to-disorder structural switch activates the FoxM1 transcription factor. *Elife* **8**, 1–25.
183 Jang S & Song JJ (2019) The big picture of chromatin biology by cryo-EM. *Curr Opin Struct Biol* **58**, 76–87.
184 Finogenova K, Bonnet J, Poepsel S, Schafer IB, Finkl K, Schmid K, Litz C, Strauss M, Benda C & Muller J (2020) Structural basis for PRC2 decoding of active histone methylation marks H3K36me2/3. *Elife* **9**, 1–30.
185 Kasinath V, Faini M, Poepsel S, Reif D, Feng XA, Stjepanovic G, Aebersold R & Nogales E (2018) Structures of human PRC2 with its cofactors AEBP2 and JARID2. *Science* **359**, 940–944.
186 Grau D, Zhang Y, Lee CH, Valencia-Sanchez M, Zhang J, Wang M, Holder M, Svetlov V, Tan D, Nudler E *et al*. (2021) Structures of monomeric and dimeric PRC2:EZH1 reveal flexible modules involved in chromatin compaction. *Nat Commun* **12**, 714.
187 Park SH, Ayoub A, Lee YT, Xu J, Kim H, Zheng W, Zhang B, Sha L, An S, Zhang Y *et al*. (2019) Cryo-EM structure of the human MLL1 core complex bound to the nucleosome. *Nat Commun* **10**, 5540.
188 Xue H, Yao T, Cao M, Zhu G, Li Y, Yuan G, Chen Y, Lei M & Huang J (2019) Structural basis of

nucleosome recognition and modification by MLL methyltransferases. *Nature* **573**, 445–449.
189 Qu Q, Takahashi YH, Yang Y, Hu H, Zhang Y, Brunzelle JS, Couture JF, Shilatifard A & Skiniotis G (2018) Structure and conformational dynamics of a COMPASS histone H3K4 methyltransferase complex. *Cell* **174**, 1117–1126.e12.
190 Millard CJ, Varma N, Saleh A, Morris K, Watson PJ, Bottrill AR, Fairall L, Smith CJ & Schwabe JW (2016) The structure of the core NuRD repression complex provides insights into its interaction with chromatin. *Elife* **5**, e13941.
191 Beck M, Mosalaganti S & Kosinski J (2018) From the resolution revolution to evolution: structural insights into the evolutionary relationships between vesicle coats and the nuclear pore. *Curr Opin Struct Biol* **52**, 32–40.
192 Casanal A, Kumar A, Hill CH, Easter AD, Emsley P, Degliesposti G, Gordiyenko Y, Santhanam B, Wolf J, Wiederhold K *et al.* (2017) Architecture of eukaryotic mRNA 3'-end processing machinery. *Science* **358**, 1056–1059.
193 Trnka MJ, Pellarin R & Robinson PJ (2019) Role of integrative structural biology in understanding transcriptional initiation. *Methods* **159–160**, 4–22.
194 Chakraborty S, Jasnin M & Baumeister W (2020) Three-dimensional organization of the cytoskeleton: A cryo-electron tomography perspective. *Protein Sci* **29**, 1302–1320.
195 Beck M & Baumeister W (2016) Cryo-electron tomography: can it reveal the molecular sociology of cells in atomic detail? *Trends Cell Biol* **26**, 825–837.
196 Dey G, Culley S, Curran S, Schmidt U, Henriques R, Kukulski W & Baum B (2020) Closed mitosis requires local disassembly of the nuclear envelope. *Nature* **585**, 119–123.
197 Booth DG, Beckett AJ, Molina O, Samejima I, Masumoto H, Kouprina N, Larionov V, Prior IA & Earnshaw WC (2016) 3D-CLEM reveals that a major portion of mitotic chromosomes is not chromatin. *Mol Cell* **64**, 790–802.
198 Sun M, Shen B, Li W, Samir P, Browne CM, Link AJ & Frank J (2021) A time-resolved Cryo-EM Study of *Saccharomyces cerevisiae* 80S ribosome protein composition in response to a change in carbon source. *Proteomics* **21**, e2000125.
199 Maeots ME, Lee B, Nans A, Jeong SG, Esfahani MMN, Ding S, Smith DJ, Lee CS, Lee SS, Peter M *et al.* (2020) Modular microfluidics enables kinetic insight from time-resolved cryo-EM. *Nat Commun* **11**, 3465.
200 Dandey VP, Budell WC, Wei H, Bobe D, Maruthi K, Kopylov M, Eng ET, Kahn PA, Hinshaw JE, Kundu N *et al.* (2020) Time-resolved cryo-EM using Spotiton. *Nat Methods* **17**, 897–900.
201 Mapelli M, Massimiliano L, Santaguida S & Musacchio A (2007) The Mad2 conformational dimer: structure and implications for the spindle assembly checkpoint. *Cell* **131**, 730–743.